Modeling the Structural Behavior of the Piston Rings under Different Boundary Conditions in Internal Combustion Engines

by

Dian Xu

B.S. Mechanical Engineering
Peking University, 2005

Submitted to the Department of Mechanical Engineering
in Partial Fulfillment of the Requirement for the Degree of

Master of Science in Mechanical Engineering

at the

Massachusetts Institute of Technology

May 2010

[June 2010]

Signature of Author______________________________
Department of Mechanical Engineering
May, 2010

Certified by______________________________
Tian Tian
Principal Research Engineer, MIT Energy Initiative
Thesis Supervisor

Accepted by______________________________
David E. Hardt
Chairman, Department Committee on Graduate Studies
Department of Mechanical Engineering

(This Page was intentionally left blank)

Modeling the Structural Behavior of the Piston Rings under Different Boundary Conditions in Internal Combustion Engines

by

Dian Xu
Submitted to the Department of Mechanical Engineering on
May 7, 2010
in Partial Fulfillment of the Requirement for the Degree of
Master of Science in Mechanical Engineering

ABSTRACT

In the process of designing internal combustion engine, piston ring plays an important role in fulfilling the requirements of camber gas sealing, friction reduction and lubrication oil consumption. The goal of this thesis is to have a better understanding of the ring behaviors under different working conditions in a structural level. This thesis is an extension of existing ring design tool. A model is built up to simulate the processes of changing ring states from one to another such as free or fit the ring. It revealed the sensitive characters of the piston ring tip; it expanded the field of application of the existing piston ring design tool; it also investigated the ring bore interaction in more conditions.

This work removed the symmetric assumption in the existing tool. A new method that calculates ring free shape and ring bore contact force from ring ovality data is introduced for the first time. The analysis of ring bore interaction is widened. The model was applied to an industry ring design case. In this case it shows the free and fit procedure in this model is physically and mathematically reversible. It shows these procedures are direction independent. The contact force distribution changes when the ring is moving within the distorted bore. It also changes when the wetting or roughness situation is different. This model can calculate the ring free shape from asymmetric measured ovality data. It can also retrieve the desired contact force from it.

The piston ring design tool is updated and implemented with these highly appreciable new features. This complete package has high efficiency and a wider practical field.

Thesis Supervisor:

Tian Tian
Principal Research Engineer, MIT Energy Initiative

(This Page was intentionally left blank)

ACKNOWLEDGEMENT

First of all, I would like to give my special thanks to Dr. Tian Tian. He not only gave me the most precious opportunity to study in MIT, he also taught me the principle and the academic way of research. His innovative thinking and the vision of the integrity of the project gives me great inspiration. He guided me through the whole master degree research process through every aspect which is a priceless fortune for me.

I would like to thank the students in the Consortium on Lubrication in Internal Combustion Engine at MIT. Haijie as a model student is always welcoming all my questions about research or academic life. Dongfang, Eric and Kia have been great helpful too. I also would like to thank all the sponsors in the consortium, especially Mahle. Without your support this work couldn't be exist.

Thanks to Yong, he has been a great mentor for me from the beginning of my MIT journey. Being a student living aboard, his help on life and study is the most appreciated. I also like to take this opportunity to thank the members in Sloan Automobile Laboratory. Thanks Professor Wai, Mr. Thane and many more. I also have to thank Mrs. Leslie in the Department. She has been nothing but enormous helpful and kind.

At last I have to thank my family, professors and friends in China. I also have to thank Ronald, Ann, Xing, and Tony, I cannot make through those stressful time without their support.

Dian Xu

May 2010

(This Page was intentionally left blank)

Table of Contents

List of Figures

Chapter 1 Introduction

Piston rings are precisely-made components which help the engine harness the energy contained in the fuel, convert it into useful power and reduce the friction that the piston encounters during the vertical reciprocating movement in the cylinder [1]. The main functions of the piston rings are to seal the combustion chamber, transfer heat to the cylinder bore and control the lubrication oil consumption.

In order to investigate the performance of the piston ring, a design tool is needed to simulate the mechanical behavior of piston ring in different working conditions and its interaction with the cylinder bore. By analyzing the ring performances such as chamber gas sealing, heat transfer and oil control, an optimized ring free shape should be calculated by this tool as a reference for ring manufacture purpose. Contrarily, this tool should be able to calculate the ring bore interaction by using the measured ring data which might include the shape of the ring and the pressure composed on the ring under different working conditions. This design tool should also be able to prove its feasibility in many ways.

The goal of this work is to develop a calculation network connecting different ring working conditions. Currently there is a ring design tool from Liang's work [2] but some design paths are missing, for example, to calculate the ring free shape from measured ring ovality data. There are many ways of designing a piston ring, which means there are many starting points that engineer can use as the input. Industry can set up certain goal such as retrieving an even ring bore contact force distribution as the starting point for design, then calculate the corresponding ring free shape. They can also base on other measured ring working conditions such as ovality state as the initial states of a design circle.

In this chapter, the goal of piston ring design is addressed first; different types of piston ring and ring states are introduced. Two common starting points of piston ring design are explained and the objectives of this thesis work are stated.

1.1 Piston Ring Design

There are several piston ring design considerations. A good design should meet certain criteria and goals.

The finished piston ring should conform to the cylinder bore well. A larger clearance between them can cause gas blow by and oil leakage and consumption; it can also increase the noise of piston. Insufficient clearance can cause the piston to seize in the cylinder and increase the friction force [3].

The assembled ring which is pressing against the cylinder wall must generate enough contact pressure that seals the high pressure combustion gas. In order to seal the combustion chamber, an inherent pressure should be applied on the ring. Generally the diameter of a free piston ring is larger than the bore. It requires a significant force to compress the piston ring to a smaller diameter so that it can be assembled in the cylinder and provides the desiring pressing pressure. This inherent pressure, or called initial internal spring force, is generated by this squeezing process and it is determined by the shape of the free ring. For example different free ring gap size can provide different inherent pressure. The bigger the gap size, the more force is needed to compress the ring and the more inherent force is, if the closed gap size is the same. The task of piston ring design is to give the free ring shape that has the desired properties. Here ring shape means the trajectory of the cross section CG of the ring.

1.2 Types of Piston Rings

Typical piston ring pack system includes three types of ring in today's automobile application.

Top ring (compression ring) as shown in figure 1-1 is the top or the closest ring to the combustion chamber. It is exposed to the combustion gas and a lot of chemical reactions. Top ring has the highest operation temperature and it also transfer most of the heat from piston to the cylinder wall. The cross section of the first ring usually is rectangular or keystone. The main function of top ring is to seal the combustion gas and provide a mild scraping behavior to prevent any excess oil from reaching the combustion chamber.

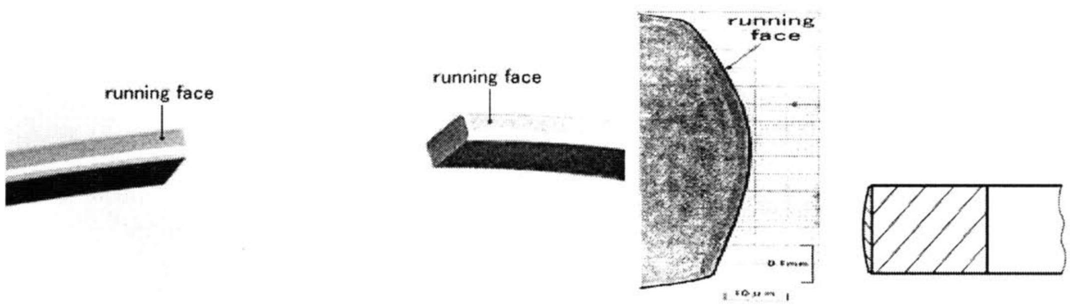

Figure 1-1 The running face and cross section of the top ring [4]

The second ring as shown in figure 1-2 is the next ring away from the piston head. It is also known as Napier ring or scraper ring. [5] The inherent tension in the second ring will give the undercut bottom side a scraping effect to scrap the oil downward and provides a consistent thickness of oil to lubricate the top ring. It also serves to complement the top ring in its sealing function. This taper face profile also allows for a fast running-in period.

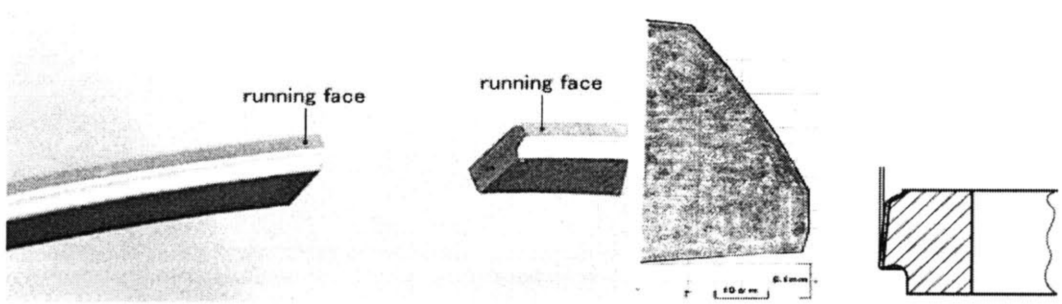

Figure 1-2 The running face and cross section of the second ring [4]

The third ring oil control ring as shown in figure 1-3 often has two lands, called twin land oil control ring. Lubricating oil is important to reduce operating friction, make the engine efficient, serve to cool critical engine components and trap harmful dirt particles. It helps the piston to slide without making direct metal to metal contact and the friction force is reduced dramatically. However, it is also desirable to keep this amount of oil to a minimum. To allow the flow of excess oil back to the oil reservoir, holes or slots are cut into the radial center of the third ring. Some of the oil control rings are utilized a spring expander, which usually contains multiple slots or windows to return oil to the piston ring groove, to apply additional radial pressure to increase the unit pressure applied at the cylinder wall.

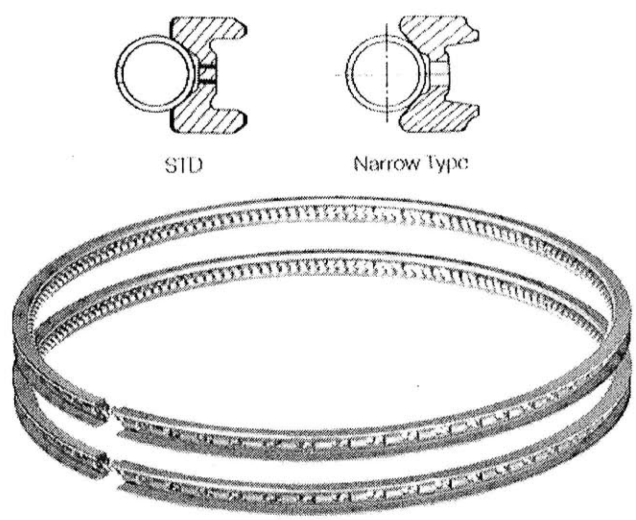

Figure 1-3 The cross section of twin land oil control ring [4]

1.3 Piston Ring in Different Working Conditions

A piston ring can be in various types of working conditions. It can be in a free state that no external force or restriction is opposed on the ring [6]. Another commonly used state is ovality state when the open joints in the periphery of the ring are closed by tightening a flexible band which packs from outer surface of the ring. After the ring is assembled into the cylinder bore and interacts with it [7], the state of the ring is called conformability state in this thesis.

Free state is the state when all the constrains and external pressure are removed from the ring, the corresponding shape is called ring free shape. Piston ring is often produced following the pattern of a well designed ring free shape. The important parameters of this state are the radius between the ring and the design center and the ring gap size. Figure 1-4 shows some common used ring free shape vocabulary.

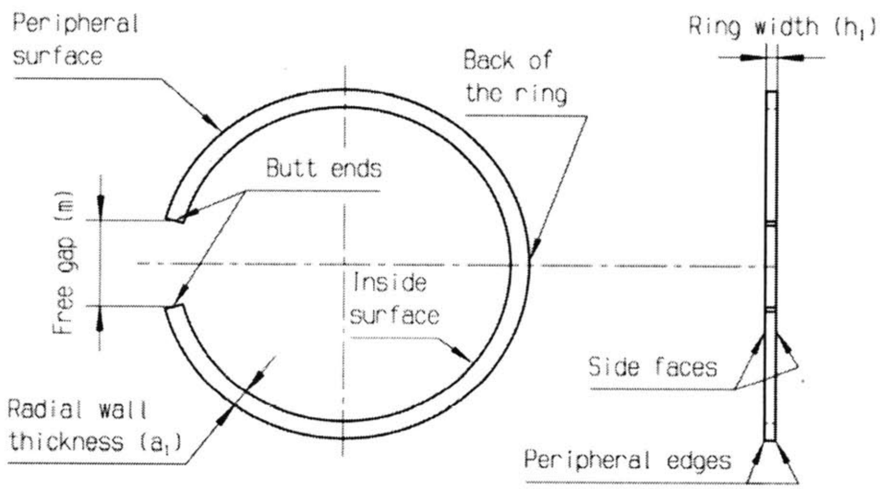

Figure 1-4 Common used free ring vocabulary [5]

Ovality state as shown in figure 1-5 is the state when the ring gaps are forcing to close by a flexible band coating on the outside surface of the ring. This ovality state is commonly seen in manufacture process because the ring shape and the force which is used to close the ring gaps are easy to measure. This force is called tangential force is the main parameter of the ovality state, also is the ovality ring shape. A very important property of the ovality state is that the pressure acting on the ring is uniformly distributed even if the ring shape is not nominal circle.

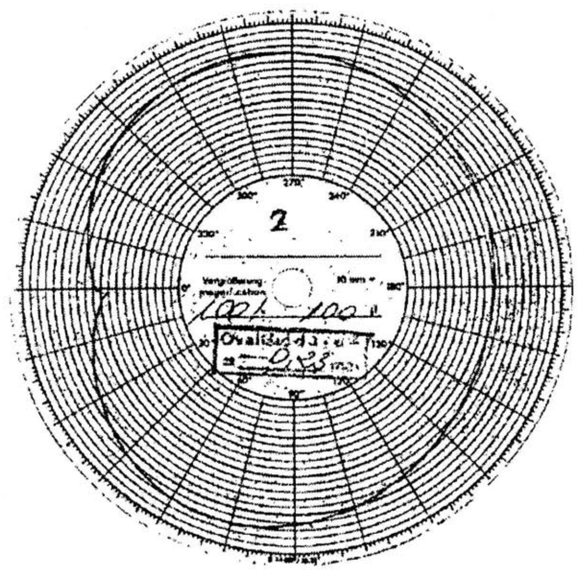

Figure 1-5 An ovality ring measurement [2]

Conformability state as shown in figure 1-6 is the state that after the ring is mounted on the piston and released to interact to the cylinder bore. Piston ring at this state can have twisting, losing contact with the bore or tilt against the wall due to the bore distortion and asymmetric characteristic of the ring cross section [2]. Contact force and ring bore clearance is important at this state for piston ring behavior analysis.

Figure 1-6 Assembled ring after interact with the bore with axial life and twist angle [2]

1.4 Starting Point of Piston Rings Design

Industry usually wants to design a piston ring that after it interacts with the cylinder bore it generates certain contact force distribution along the circumference, for example, an even contact force distribution. The question is that based on this initial ring state, how we can find the corresponding ring free shape. Once the piston ring following this free shape design is produced, after it is assembled back into the cylinder, the desired even contact force distribution should be retrieved as it is designed in such way. Some other types of initial force distribution are also used as shown in figure 1-7. What types of contact force distribution to choose is determined by the related simulation results such as oil consumption or ring bore conformability.

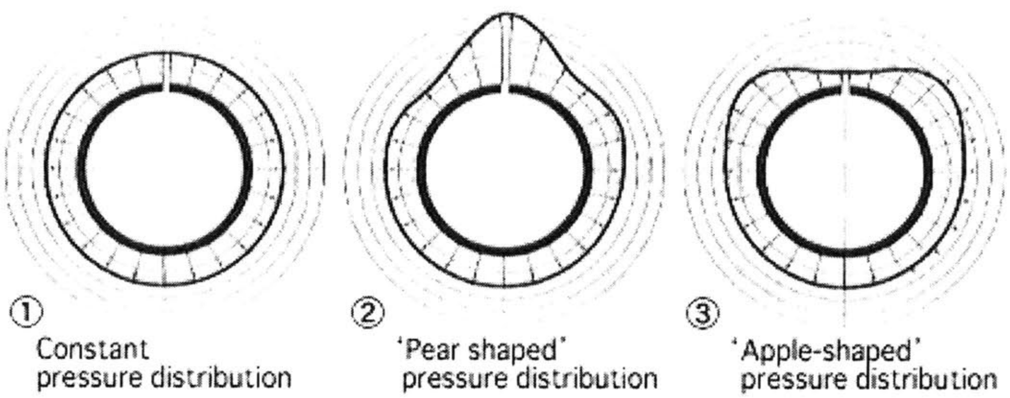

Figure 1-7 Various types of desired piston ring contact pressure distribution [4]

Assuming the ring free shape is calculated and the ring is finally made, what industry usually does is to close the free ring into ovality state then measure the requiring tangential load and the ovality shape. This is because tangential load and ring ovality are two important ring properties. The method of measuring ovality shape is mature and the data are easy to get. It is nature to use these ovality data to do ring analysis, for example, calculating the ring free shape or contact force. Then these results can give valuable feedback to the design. The challenge here is that ovality state is usually asymmetric which the existing tool cannot handle.

1.5 Objectives of the Thesis Work

The existing piston ring design tool developed by Liu can be used in a very wide range of application [8, 9]. The major functions are [2]:

1. Given theoretical contact force, calculate the ring free shape;
2. Given theoretical ring free shape, calculate the contact force;
3. Given theoretical ring free shape, calculate the ovality shape.

There are some limitations of the existing tool:

1. The given input information such as theoretical contact force or ring free shape must be symmetric, the procedures as free or fit the ring need to fix the symmetric center of the ring, ring back;
2. If given ovality data, it cannot calculate the ring free shape;

The challenge is all the measured ring data in industry are asymmetric, either the measured ring free shape or ovality shape. If we can remove this symmetric restriction, the ring design tool can be used in a much larger region. This also means that theoretically we can deal with any type of ring shape under any type of pressure distribution.

Another challenge is how to simulate the ring behavior from ovality shape. Since the ovality shape data are often used in industry, there is an urgent need for the simulation that uses ovality data as input. Once we can calculate the ring free shape from ovality, the related contact force can also be calculated. This contact force can be used to compare with the desire contact force in design stage. Thus a calculation network can be developed. Each node in this network can validate or give reflection of whether the initial design is good or not.

Based on these considerations, the objectives of this work are:

1. Remove the symmetric assumption from the existing tool so that the tool can be used on arbitrary ring under certain pressure distribution, especially on the industry measured data;
2. Calculate the ring free shape from the ovality shape, then calculate the related ring bore interactions such as contact force and clearance;

3. Build a calculation network connecting different ring states: free state, ovality state and conform state.

During the process of developing this new tool, we also discovered some important ring characteristics in structural level:

1. Ring tip is very sensitive to many situations. Small amount of error near the ring tip region can contribute huge difference to the final result such as contact force. Such situations are: the location of the ring tip, the way of calculating the curvature near ring tip and the position of the nominal bore where the ring is put at;
2. In the process of handling the ring, certain procedure such as free and fit (which will be addressed later) must be reversible, if not the procedure will lose its credibility;
3. Changing the environment between the ring running surface and the cylinder bore can affect the contact force in several ways. For example: rotating the ring, ring moves reciprocate within the bore, changing ring bore roughness and changing lubrication oil distribution.

The combination of these objectives will come with an analytic numerical package that can be used to analyze the ring behavior from different ring initial states and validate these behaviors in different ways. And these ring characteristics will play an important role in building up the model; they also give the basic assumption.

Chapter Two will discuss how to discretize the piston ring and its pressure distribution. FEM will be used and the method will be explained briefly. A 3D version of beam element will be chosen as our model. The issues, which need special attention related to the discretized piston ring will be explained. Chapter Three explains two major procedures we used to change the ring state: free procedure and fit procedure. How they are carried out will be discussed in detail. Additionally, the choice of bore position and the equivalence of these two procedures are also addressed. Chapter Four is focusing on ring bore interactions. Two models: asperity contact force model and hydrodynamics lubrication model are explained. The conformability calculation is explained. By changing the ring environment such as rotating\moving the ring within the bore, changing roughness and oil distribution, we can show how the ring reacts to them. Chapter Five will give an industry application to show how this new model works.

(This Page was intentionally left blank)

Chapter 2 Discretization of the Ring

2.1 Introduction

In this chapter, as the first step of mechanical analysis, the piston ring is discretized into discontinuous elements. A 3-D straight beam element is used in considering the slender character of the ring. The local coordinate and the DOF (degree of freedom) are set up. The continuous initial pressure distribution is also discretized. The way how the global stiffness matrix is assembled is explained. The mathematical foundation of straight beam model is described. At the end, a discretized ring free/fit procedure is recapped [2].

To analyze the mechanical behavior of the piston ring in a structural level, the first step is discretization. A proper type of element should be chosen to discretize the ring. From geometry wise, this type of element should be precise enough to represent the changing of the shape of the ring. From physics wise, the continuous pressure acting on these elements should be discretized into discontinuous node forces which are still in mechanical balance.

Straight beam model is used in the following analysis. This type of element mainly supports compressing, stretching and twisting in axial direction and transverse bending moment [10]. The relation between displacement and force is developed with stiffness matrix. After carefully chosen the local node direction, a global stiffness matrix can be expressed which will be used together with the proper DOF set up to solve the displacement and force vector.

When the ring state changes from one to another, for example from ovality state to free state, the displacement of certain node points are very large. In order to use the classic FEM which is based on small displacement assumption, a discretized procedure should also be introduced in order to prevent large displacement during the procedure. A step-by-step method [2] is used here. Taking free procedure for example, instead of freeing all the nodes at a time, one node is released at a time. When the force and moment are balanced again, the next node is released [2]. This will guarantee each step the shift of the ring shape is under small displacement restriction.

2.2 Geometry Discretization

For the first step, the piston ring is divided into many elements in circumferential direction. Because the length of typical piston rings in cross section direction is much smaller than the length in the circumferential direction, a beam element model should be suitable here. Each element of the ring is considered as a straight beam which is a slender member that is used for supporting transverse loading. 3-D straight beam element model is used with the virtue of suitability and high calculation efficiency [11]. Beam element model requires that the length of the element's axial direction should be three times larger than that in the cross section direction. Follow this criterion a reasonable mesh size is chosen to discretize the ring.

The setup of the DOF of each node is important. Displacement freedom in circumferential direction allows the element free from compression or stretching; the displacement in radius direction determines whether the element is tilting away or bending inward to the bore. Also the bending angle decides the local curvature of the ring; the twisting angle shows how the ring behaves under either asymmetrical cross section condition or distorted bore environment. The common part of DOF set up of the two mean procedures which will be explained in next chapter is:

1. Nodes are allowed to move in circumferential direction;
2. Cross section is allowed to bend freely.

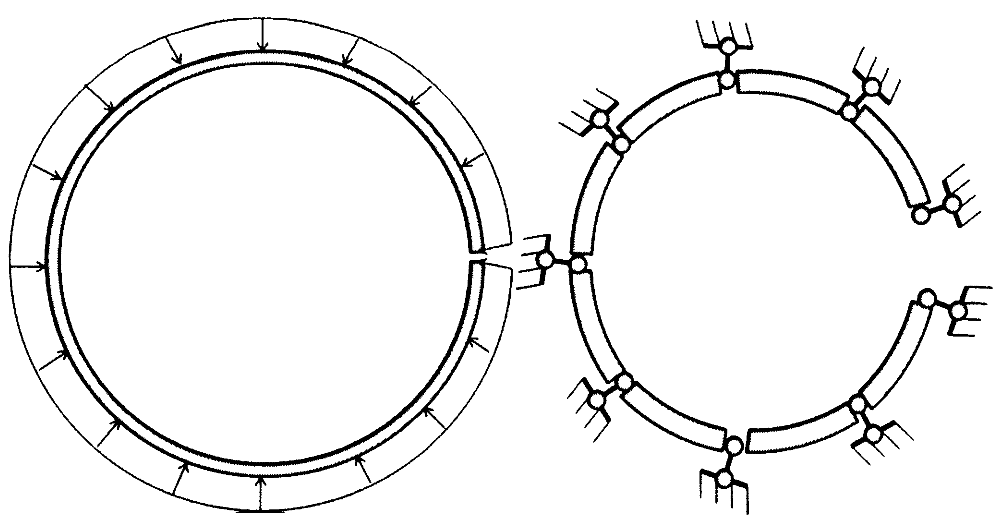

Figure 2-1 Ring geometry discretization (before vs. after)

2.3 Force Discretization

The piston ring is under continuous pressure distribution. This continuous pressure needs to be discretized into node force. Figure 2-2 shows the even pressure distribution condition. There are two elements at each sides of the node point. For the left side element, the pressure on the right half of the element is chosen, so does the left half of the right side element. Then the pressure integral of this region in this case which is force times element length is calculated as the node force acting on the support of the node. Figure 2-3 shows the case that the two adjacent elements are not in the same direction. In this case the average force value and direction of these two elements are taken as the node force [12].

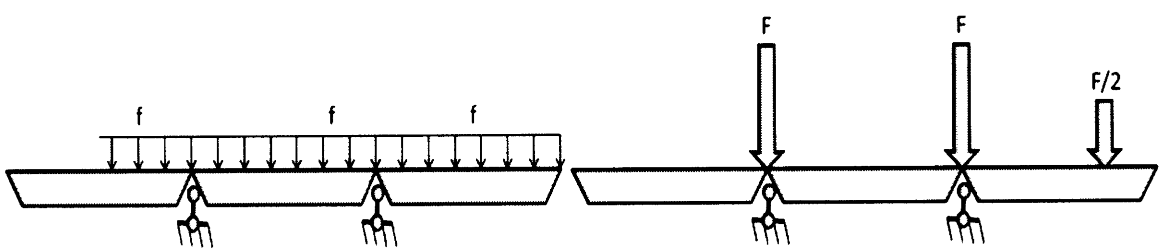

Figure 2-2 Force discretization when the directions are the same on two elements (before vs. after)

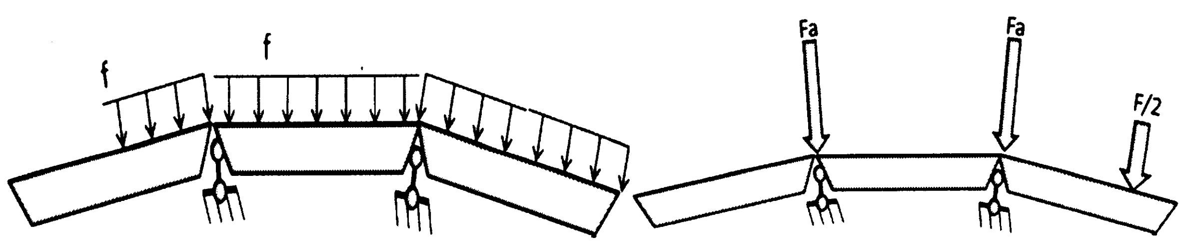

Figure 2-3 Force discretization when the directions are different on two elements (before vs. after)

Figure 2-4 shows a non-uniform pressure distribution case. As it shows the integral of the pressure distributed on both halves of two elements are takes as node force.

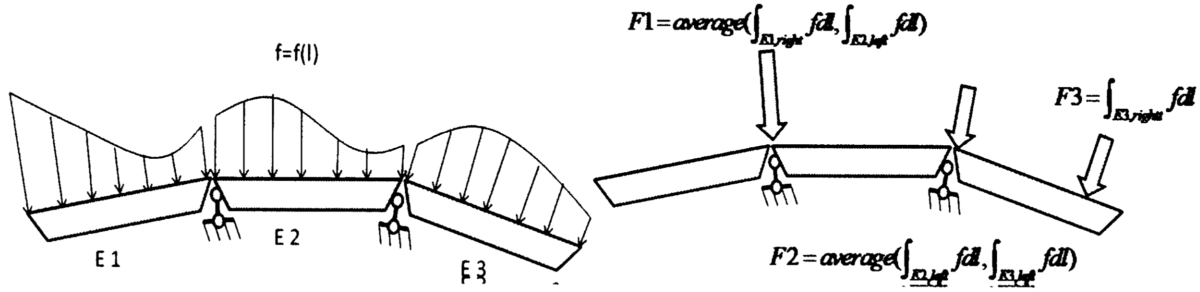

Figure 2-4 Force discretization when the continuous pressure is non-uniform

At the node points of ring gaps, taking an even pressure distribution for example, the converted node forces should be half of the other node forces since there is only half element left for discretization. Because of the existence of the ring gap, the actual node force should be bigger in order to maintain force balance:

$$F/2(\cos\alpha) \Rightarrow F/2 \tag{2.1}$$

Where α is half of the ring gap angle, F is the force on other nodes rather than tip nodes as shown in figure 2-5, the ring is balanced by these forces.

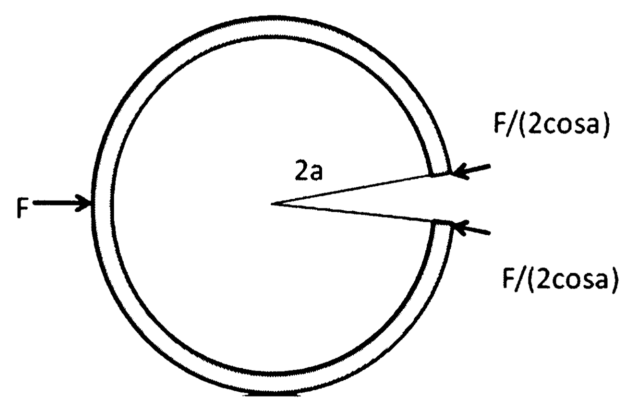

Figure 2-5 Ring tip node force modification

2.4 Displacement and force

Each beam element has 12 displacements, correspondingly there are 12 forces acting on these directions. The relationship between displacement and force is established on Galerkin's Method [10]. Three groups of independent relations are explained as below.

Stretch/Compress [13]:

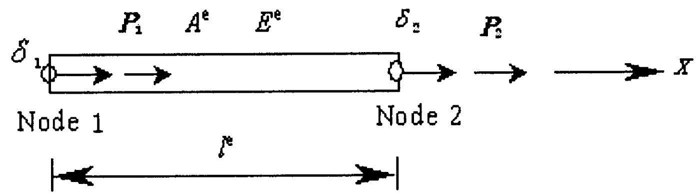

Figure 2-6 Stretch/Compress of a beam element

As shown in figure 2-6, the element is under stretching/compressing. Displacement vector and force vector of these two nodes named Node1 and Node2 are:

$$q^e = [\delta_1 \quad \delta_2]^T, P^e = [\delta_1 \quad \delta_2]^T \tag{2.2}$$

Assuming the relation between nodes displacements and element displacement field is:

$$u^e(x) = a_0 + a_1 x \tag{2.3}$$

We have the relationship between the displacement field and node force:

$$u^e(x) = [1 - x/l^e \quad x/l^e] \cdot q^e \tag{2.4}$$

Corresponding strain field and stress field is:

$$\begin{aligned} \varepsilon^e(x) &= \frac{du^e(x)}{dx} = [-1/l^e \quad 1/l^e] \cdot q^e \\ \sigma^e(x) &= E^e \cdot \varepsilon^e(x) \end{aligned} \tag{2.5}$$

Element potential energy can be written as:

$$\Pi^e = \frac{1}{2}\int_0^{l^e} \sigma^e(x)\cdot\varepsilon^e(x)\cdot A^e dx - P^{eT}\cdot q^e = \frac{1}{2}q^{eT}\cdot K^e\cdot q^e - P^{eT}\cdot q^e \tag{2.6}$$

Where the element stiffness matrix is:

$$K^e = \frac{E^e A^e}{l^e}\begin{bmatrix} 1 & -1 \\ -1 & 1 \end{bmatrix} \tag{2.7}$$

Where E is the Young's module, A is the area of the cross section, l is the element length.

Bending: [13]

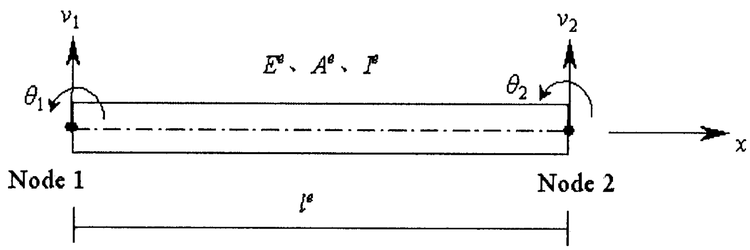

Figure 2-7 Bending of a beam element

As shown in figure 2-7, the element is under bending. Displacement vector and force vector of these two nodes named Node1 and Node2 are:

$$q^e = [v_1 \quad \theta_1 \quad v_2 \quad \theta_2]^T, P^e = [P_{1v} \quad M_1 \quad P_{2v} \quad M_2]^T \tag{2.8}$$

Assuming the relation between nodes displacements and element displacement field is:

$$v^e(x) = a_0 + a_1 x + a_2 x^2 + a_3 x^3 \tag{2.9}$$

We have the relationship between the displacement field and node force:

$$v^e(x) = [(1-3\xi^2+2\xi^3) \quad l^e(\xi-2\xi^2+\xi^3) \quad (3\xi^2-2\xi^3) \quad l^e(\xi^3-\xi^2)]\cdot q^e \tag{2.10}$$

Corresponding strain field and stress field is:

$$\begin{aligned} \varepsilon^e(x,\hat{y}) &= -\hat{y}\frac{d^2 v^e(x)}{dx^2} = -\hat{y}[(12\xi-6)/l^{e2} \quad (6\xi-4)/l^e \quad -(12\xi-6)/l^{e2} \quad (6\xi-2)/l^e]\cdot q^e \\ \sigma^e(x) &= E^e\cdot\varepsilon^e(x) \end{aligned} \tag{2.11}$$

Element potential energy can be written as:

$$\Pi^e = \frac{1}{2} q^{eT} \cdot K^e \cdot q^e - P^{eT} \cdot q^e \tag{2.12}$$

Where the element stiffness matrix is:

$$K^e = \frac{E^e I_z}{l^{e3}} \begin{bmatrix} 12 & 6l^e & -12 & 6l^e \\ 6l^e & 4l^{e2} & -6l^e & 2l^{e2} \\ -12 & -6l^e & 12 & -6l^e \\ 6l^e & 2l^{e2} & -6l^e & 4l^{e2} \end{bmatrix} \tag{2.13}$$

where I is the principle moment of inertia.

Twisting: [10]

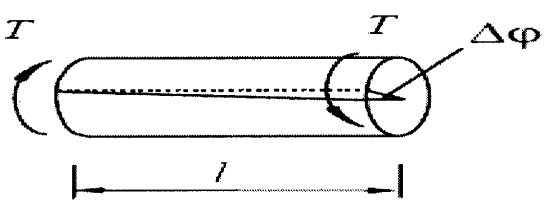

Figure 2-8 Twisting of a beam element

As shown in figure 2-8, the element is under twisting. Displacement vector and force vector of these two nodes named Node1 and Node2 are:

$$q^e = [\varphi_1 \quad \varphi_2]^T, P^e = [M_{z1} \quad M_{z2}]^T \tag{2.14}$$

Element potential energy can be written as:

$$\Pi^e = \frac{1}{2} q^{eT} \cdot K^e \cdot q^e - P^{eT} \cdot q^e \tag{2.15}$$

Where the element stiffness matrix is:

$$K^e = \frac{G^e J^e}{l^e} \begin{bmatrix} 1 & -1 \\ -1 & 1 \end{bmatrix} \tag{2.16}$$

Where G is the Twisting module, J is the torsion factor.

Assembly three working conditions together as shown in figure 2-9:

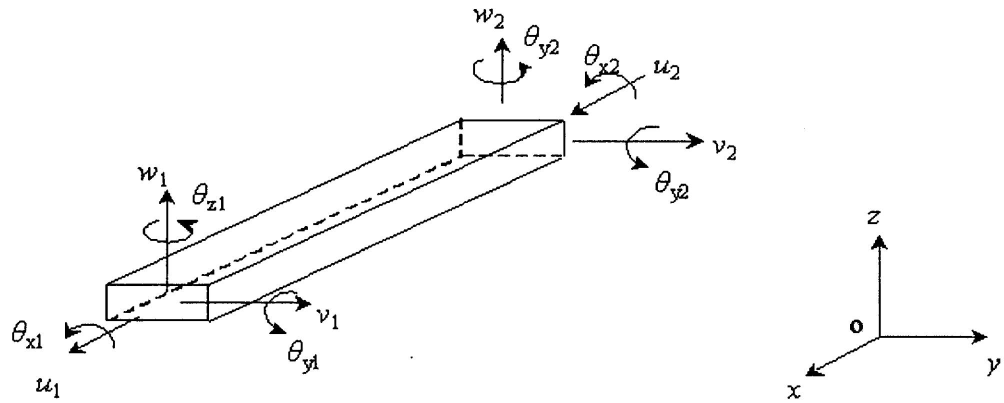

Figure 2-9: 3-D beam element displacements

Displacement vector and force vector of these two nodes named Node1 and Node2 are:

$$\underset{(12\times1)}{\mathbf{q}^e} = \begin{bmatrix} u_1 & v_1 & w_1 & \theta_{x1} & \theta_{y1} & \theta_{z1} & u_2 & v_2 & w_2 & \theta_{x2} & \theta_{y2} & \theta_{z2} \end{bmatrix}$$

$$\underset{(12\times1)}{\mathbf{P}^e} = \begin{bmatrix} P_{u1} & P_{v1} & P_{w1} & M_{x1} & M_{y1} & M_{z1} & P_{u2} & P_{v2} & P_{w2} & M_{x2} & M_{y2} & M_{z2} \end{bmatrix} \tag{2.17}$$

We can have the stiffness matrix for a single beam element assembled as: [13]

$$\underset{(12\times12)}{\mathbf{K}^e} = \begin{bmatrix}
\frac{EA}{l^e} & 0 & 0 & 0 & 0 & 0 & -\frac{EA}{l^e} & 0 & 0 & 0 & 0 & 0 \\
0 & \frac{12EI_z}{l^{e3}} & 0 & 0 & 0 & \frac{6EI_z}{l^{e2}} & 0 & -\frac{12EI_z}{l^{e3}} & 0 & 0 & 0 & \frac{6EI_z}{l^{e2}} \\
0 & 0 & \frac{12EI_y}{l^{e3}} & 0 & -\frac{6EI_y}{l^{e2}} & 0 & 0 & 0 & -\frac{12EI_y}{l^{e3}} & 0 & -\frac{6EI_y}{l^{e2}} & 0 \\
0 & 0 & 0 & \frac{GJ}{l^e} & 0 & 0 & 0 & 0 & 0 & -\frac{GJ}{l^e} & 0 & 0 \\
0 & 0 & -\frac{6EI_y}{l^{e2}} & 0 & \frac{4EI_y}{l^e} & 0 & 0 & 0 & \frac{6EI_y}{l^{e2}} & 0 & \frac{2EI_y}{l^e} & 0 \\
0 & \frac{6EI_z}{l^{e2}} & 0 & 0 & 0 & \frac{4EI_z}{l^e} & 0 & -\frac{6EI_z}{l^{e2}} & 0 & 0 & 0 & \frac{2EI_z}{l^e} \\
-\frac{EA}{l^e} & 0 & 0 & 0 & 0 & 0 & \frac{EA}{l} & 0 & 0 & 0 & 0 & 0 \\
0 & -\frac{12EI_z}{l^{e3}} & 0 & 0 & 0 & -\frac{6EI_z}{l^{e2}} & 0 & \frac{12EI_z}{l^{e3}} & 0 & 0 & 0 & -\frac{6EI_z}{l^{e2}} \\
0 & 0 & -\frac{12EI_y}{l^{e3}} & 0 & \frac{6EI_y}{l^{e2}} & 0 & 0 & 0 & \frac{12EI_y}{l^{e3}} & 0 & \frac{6EI_y}{l^{e2}} & 0 \\
0 & 0 & 0 & -\frac{GJ}{l^e} & 0 & 0 & 0 & 0 & 0 & \frac{GJ}{l^e} & 0 & 0 \\
0 & 0 & -\frac{6EI_y}{l^{e2}} & 0 & \frac{2EI_y}{l^e} & 0 & 0 & 0 & \frac{6EI_y}{l^{e2}} & 0 & \frac{4EI_y}{l^e} & 0 \\
0 & \frac{6EI_z}{l^{e2}} & 0 & 0 & 0 & \frac{2EI_z}{l^e} & 0 & -\frac{6EI_z}{l^{e2}} & 0 & 0 & 0 & \frac{4EI_z}{l^e}
\end{bmatrix} \tag{2.18}$$

2.5 Coordinate Transformation

The nodes displacements in local coordinate can be written as:

$$\underset{(12\times1)}{\mathbf{q}^e} = [u_1 \quad v_1 \quad w_1 \quad \theta_{x1} \quad \theta_{y1} \quad \theta_{z1} \quad u_2 \quad v_2 \quad w_2 \quad \theta_{x2} \quad \theta_{y2} \quad \theta_{z2}]^T \tag{2.19}$$

Let:

$$\underset{(12\times1)}{\overline{\mathbf{q}}^e} = [\overline{u}_1 \quad \overline{v}_1 \quad \overline{w}_1 \quad \overline{\theta}_{x1} \quad \overline{\theta}_{y1} \quad \overline{\theta}_{z1} \quad \overline{u}_2 \quad \overline{v}_2 \quad \overline{w}_2 \quad \overline{\theta}_{x2} \quad \overline{\theta}_{y2} \quad \overline{\theta}_{z2}]^T \tag{2.20}$$

to be the nodes displacement in global coordinate.

We have:

$$\begin{aligned} \overline{q}^{eT} &= T^{eT} \cdot q^{eT}, \\ \overline{P}^{eT} &= T^{eT} \cdot P^{eT}, \\ \overline{K}^{eT} &= T^{eT} \cdot K^{eT} \cdot T^e \end{aligned} \tag{2.21}$$

Where:

$$\underset{(12\times12)}{\mathbf{T}} = \begin{bmatrix} \underset{(3\times3)}{\lambda} & 0 & 0 & 0 \\ 0 & \underset{(3\times3)}{\lambda} & 0 & 0 \\ 0 & 0 & \underset{(3\times3)}{\lambda} & 0 \\ 0 & 0 & 0 & \underset{(3\times3)}{\lambda} \end{bmatrix}, \quad \underset{(3\times3)}{\lambda} = \begin{bmatrix} \cos(x,\overline{x}) & \cos(x,\overline{y}) & \cos(x,\overline{z}) \\ \cos(y,\overline{x}) & \cos(y,\overline{y}) & \cos(y,\overline{z}) \\ \cos(z,\overline{x}) & \cos(z,\overline{y}) & \cos(z,\overline{z}) \end{bmatrix} \tag{2.22}$$

So the stiffness equation is written as [13]:

$$\overline{K}^e \cdot \overline{q}^e = \overline{P}^e \tag{2.23}$$

The definition of local coordinate system for a freed element is different than the fixed one, as shown in figure 2-10. For freed node, the x axial of the local coordinate is the same direction of the element; for the fixed node, the y axial of the local coordinate is pointing towards the nominal bore center.

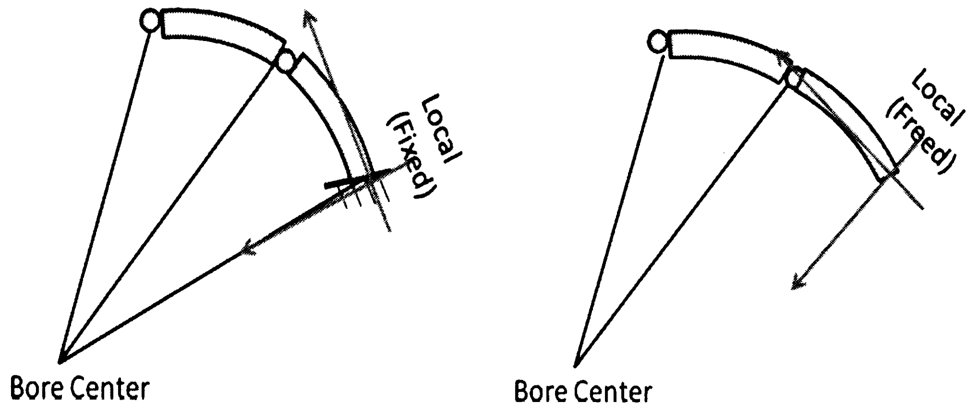

Figure 2-10: Local coordinate definition of fixed node and freed node

2.6 Global Stiffness Matrix and Boundary Conditions

The next step is to assemble the global stiffness matrix from the elements matrixes: [14]

$$\begin{pmatrix} E_{i1} & E_{i2} \\ E_{i3} & E_{i4} \end{pmatrix} \rightarrow \begin{pmatrix} E_{11} & E_{12} & & & \\ E_{13} & E_{14}+E_{21} & \cdots & & \\ & \cdots & \cdots & \cdots & \\ & & \cdots & \cdots & \cdots \\ & & & \cdots & E_{n4} \end{pmatrix} = K \tag{2.24}$$

The force vector also needs to be assembled:

$$F \leftarrow \sum_e (f^e + T^e) + P \tag{2.25}$$

Then we have:

$$\Pi = \frac{1}{2} Q^T K Q - Q^T F \tag{2.26}$$

Note that K is a symmetric matrix. The potential energy can be written in expanded form as: [6]

$$\begin{aligned} \Pi = \frac{1}{2}(&Q_1 K_{11} Q_1 + Q_1 K_{12} Q_2 + \ldots + Q_1 K_{1N} Q_N \\ &+ Q_2 K_{21} Q_1 + Q_2 K_{22} Q_2 + \ldots + Q_2 K_{2N} Q_N \\ &\ldots\ldots\ldots \\ &+ Q_N K_{N1} Q_1 + Q_N K_{N2} Q_2 + \ldots + Q_N K_{NN} Q_N) \\ &- Q_1 F_1 + Q_2 F_2 + \ldots + Q_N F_N \end{aligned} \tag{2.27}$$

Then the boundary condition is substituted into the expression above, we obtain:

$$\begin{aligned} \Pi = \frac{1}{2}(&a_1 K_{11} Q_1 + a_1 K_{12} Q_2 + \ldots + a_1 K_{1N} Q_N \\ &+ Q_2 K_{21} a_1 + Q_2 K_{22} Q_2 + \ldots + Q_2 K_{2N} Q_N \\ &\ldots\ldots\ldots \\ &+ Q_N K_{N1} a_1 + Q_N K_{N2} Q_2 + \ldots + Q_N K_{NN} Q_N) \\ &- a_1 F_1 + Q_2 F_2 + \ldots + Q_N F_N \end{aligned} \tag{2.28}$$

The displacement has been eliminated in the potential energy expression. Following the requirement that a minimum value implies that:

$$\frac{d\Pi}{dQ_i} = 0, i = 2,3,...N \tag{2.29}$$

We obtain:

$$\begin{aligned} K_{22}Q_2 + ... + K_{2N}Q_N &= F_2 - K_{21}a_1 \\ K_{32}Q_2 + ... + K_{3N}Q_N &= F_3 - K_{31}a_1 \\ \cdots\cdots\cdots \\ K_{N2}Q_2 + ... + K_{NN}Q_N &= F_N - K_{N1}a_1 \end{aligned} \tag{2.30}$$

The final FEM equations can be written as:

$$\begin{pmatrix} K_{22} & K_{23} & \cdots & K_{2N} \\ K_{32} & K_{32} & \cdots & K_{3N} \\ \cdots & \cdots & \cdots & \cdots \\ K_{N2} & K_{N3} & \cdots & K_{NN} \end{pmatrix} \begin{pmatrix} Q_2 \\ Q_3 \\ \cdots \\ Q_N \end{pmatrix} = \begin{pmatrix} F_2 - K_{21}a_1 \\ F_3 - K_{31}a_1 \\ \cdots \\ F_N - K_{N1}a_1 \end{pmatrix} \tag{2.31}$$

And the reaction load can be calculated as:

$$R_1 = K_{11}Q_1 + ... + K_{1N}Q_N - F_1 \tag{2.32}$$

Since then the displacement vector, force vector and the reaction loads are all calculated.

The matrix of this equation is symmetrically banded; we use skyline solution to store the matrix and LU decomposition to solve the equation. [14]

2.7 Step-by-Step Ring Free/Fit Procedure

As figure 2-11 shows that the displacement during the procedure of free/fit the ring is quite large especially near the freed tip. Obviously it doesn't obey the small displacement restriction of FEM. In order to restrict the shifting of the ring shape in a small amount of changing, a step-by-step procedure is used here [2]. This method is widely used in FEM to solve large displacement problem. Taking ring fit procedure for example, the solid line with node points on it is the ring free shape; the dotted line is the nominal bore that we want to fit the ring to. The basic idea is that fix one of the ring tip at the nominal bore first; the node next to it will be fit into the nominal bore. As shown in the figure the displacement at this step is small. Then this node is fixed in radius direction, the corresponding reaction load and the displacement field will be calculated and used as the initial state of the next step: fitting the next node point. Iterate this procedure until the other ring tip is fitted into the bore. It can be seen as a discretized procedure.

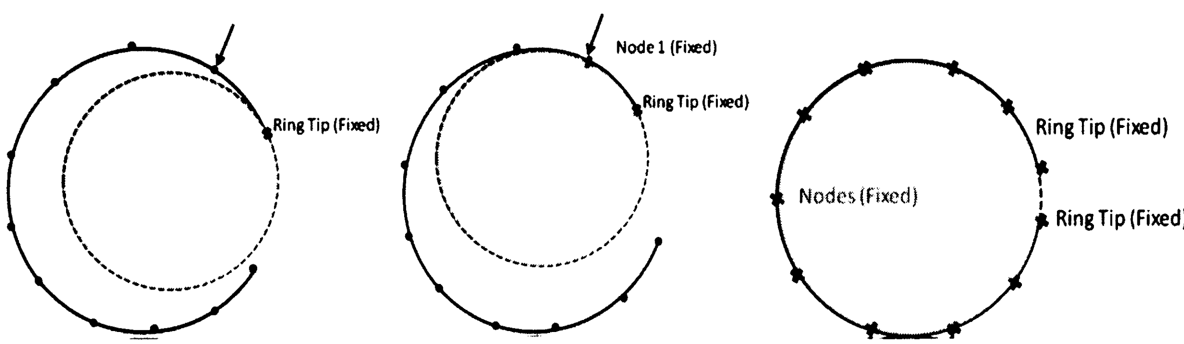

Figure 2-11 Step-by-step ring fit procedure

2.8 Conclusions

In this chapter, the geometry of the ring is discretized by a 3-D beam element because this type of element in FEM can efficiently describe the ring structural behavior. The DOF of the mesh nodes is set up in order to allow the node points move in circumferential direction and bend freely.

The initial pressure distribution on the ring is discretized also under the requirement that the force and moment should always be balanced. The ring tip elements should pay attention to because the existence of ring gap. The way of treating non-uniform pressure distribution is taking the pressure integral on both half elements on each side to be the node force.

The relationship between displacement and a single type of external force of the beam element is explained in a mathematical way. The global stiffness matrix is assembled by local element stiffness matrixes on which the coordinate transformation are preformed. The definition of local coordinate is different for fixed nodes and freed nodes.

The final global FEM equations are set up and solved using LU deposition. How to apply the known boundary conditions which are constrains in the matrix solving is also explained. Finally a step by step free or fit procedure is used because by this mean the ring can avoid large displacement in a single calculation step so that the FEM can be valid.

Chapter 3 Ring Free/Fit Procedures

3.1 Introduction

After the piston ring is discretized, FEM can be used to change the state of the ring. For instance the ring can be freed from its ovality state to free state; the free state can also be fitted into a nominal bore. The purpose of these two procedures is to get the ring prepared for the next simulation step: interacting with the cylinder bore.

The function of free procedure is to simulate the process that removing all the restrains and pressure that opposing on the piston ring. It will eventually generate a ring shape which has no external pressure nor restrains. This shape is called ring free shape. The purpose of free procedure is to calculate a ring manufacture reference. If a theoretical pressure distribution ring is freed, the ring made in this free shape is supposed to have the same pressure distribution after it is assembled into the nominal bore. Also, if the ovality ring is freed, after the free shape is closed by a flexible band, it should have the same ovality.

The function of fit procedure is to simulate the process that fitting the free ring into a nominal bore shape. It will generate an intermediate ring state which has certain restrains on the ring node points and fitting force that maintain the geometry of the ring as same as the nominal bore. The purpose of fitting procedure is to give an initial state for ring bore interaction analysis. The reason of doing this is that we cannot simply insert a free ring or an ovality ring into the bore because the shapes are very different, which will break the small displacement requirement in FEM. Instead we can easily insert this intermediate ring into the bore because the only geometry different between the bore shape and the fitted ring is bore distortion which is relatively small. The fitted ring can be achieved from free ring within limited steps of small displacement shifting.

The initial restrained ring shape or its pressure distribution doesn't have to be symmetric anymore. This is due to the ring tip curvature assumption which is a basic assumption in this thesis work. The choice of bore position will obey this assumption which will be issued below.

These two procedures are physically reversible. Some validating methods are taken to prove this point mathematically.

3.2 Bore Position

The position of the nominal bore is important to bore free and fit procedures. As the research shows, the behavior of the piston ring, especially around the ring tip, is very sensitive to where we put the bore. Figure 3-1 illustrates that different bore position can result in very different fitting force.

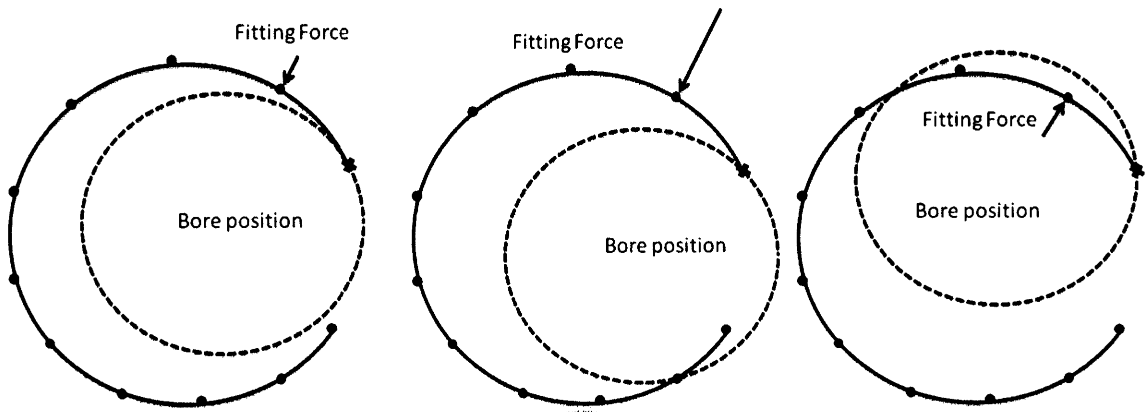

Figure 3-1 Differernt bore position results in different fitting force

The existing tool chooses to place the nominal bore at the back of the ring, as shown in Figure 3-2. Because there is a symmetric restriction in the existing tool, the ring back is defined as the symmetric center of the ring. It is also the symmetric center of the pressure distribution. By placing the bore at the ring back, and fixing ring back node at the same time [2], we can actually take only half of the ring to run the simulation.

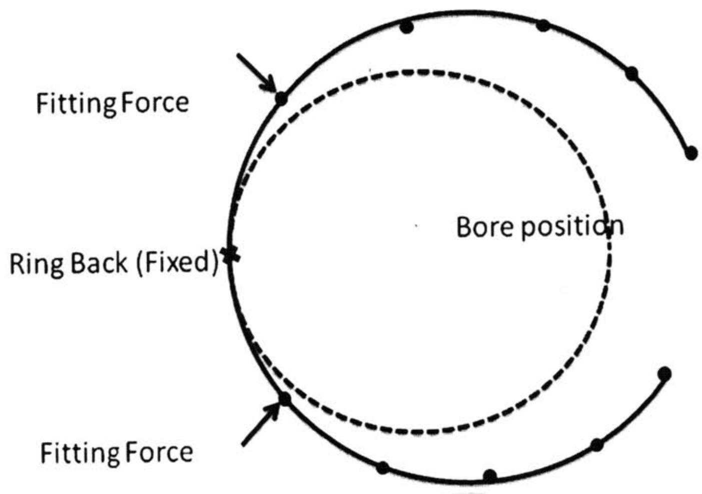

Figure 3-2 Bore position: at the ring back

The tool this thesis developed will put the bore at the ring tip, as shown in figure 3-3. The bore diameter is known, the information of the ring tip node and the node next to it is also known. If we assume the element between tip node 1 and tip node 2 has the same curvature as the nominal bore, the center of the nominal bore then can be calculated.

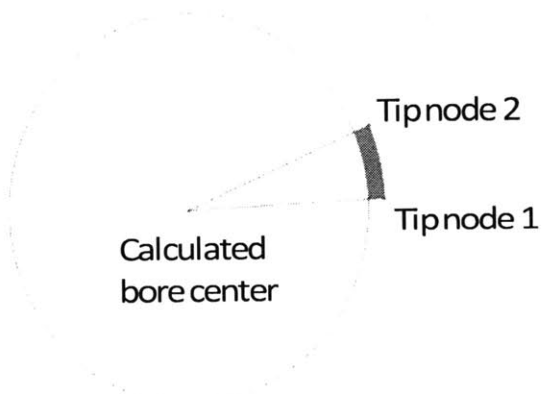

Figure3-3 Bore position: at the ring tip

Here we introduced a basic assumption in this thesis that the ring tip element has the same curvature as the nominal bore. As a matter of fact, ring tips cross sections always have no internal or external stress. Therefore the elements near the ring tips have very small pressure distribution. In other word, there is little force near the ring tip to change the shape of it. In fact it doesn't change much during most types of ring working conditions. If the ring is in the intermediate state mentioned above, which is fitted ring, the curvature of the ring tip is the same as the nominal bore. Since these state changes, which might be free or interact with the bore or close by flexible band, will have negligible impact on the curvature near the ring tip; we can assume that the curvature of the ring tip are the same in different ring states. And the boundary condition at the fixed ring tip is: position and tangential direction are fixed.

Since the node point near the ring tip is placed on the bore, the fitting force of the first step is zero, as shown in figure 3-4.

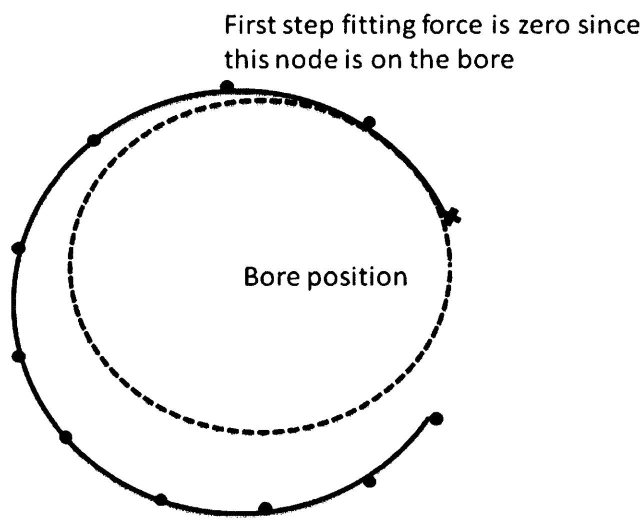

Figure 3-4 Ring tip bore position and the fitting force

Based on this assumption, the symmetric requirement is removed. Any ring shape under any pressure distribution can be used as the initial state for free/fit procedure.

3.3 Free Procedure

The ring is under certain pressure distribution and constrains, and the geometry of the ring is known too which can be asymmetric. An important task is to calculate the shape of the ring when all the pressure and constrains are removed. The purposes of doing this are: giving a free ring profile for production; giving an initial state for the following fitting procedure.

At the beginning, all the node points are fixed. All nodes have node force which is discretized from pressure acting on them. As the first step, one of the ring tips is freed in radius direction. This is done by posing a same large force but with opposite direction on the node. As shown in the equation below, F_1 is the force.

$$\begin{vmatrix} K_{11} & K_{12} & & & 0 \\ K_{13} & K_{14}+K_{21} & K_{22} & & \\ & K_{23} & \cdots & & \\ & & & \cdots & K_{n3} \\ 0 & & & K_{n2} & K_{n4} \end{vmatrix} \begin{vmatrix} u_{1,1} \\ u_{1,2} \\ \cdots \\ \cdots \\ u_{n,12} \end{vmatrix} = \begin{vmatrix} -F_1 \\ 0 \\ \cdots \\ \cdots \\ 0 \end{vmatrix} \tag{3.1}$$

The displacement vector u can be calculated to update the nodes' coordinate; the reaction load is then calculated to update the initial node force:

$$\begin{vmatrix} -F_1 \\ F_{r1,2} \\ \cdots \\ \cdots \\ F_{rn,12} \end{vmatrix} + \begin{vmatrix} F_1 \\ F_2 \\ \cdots \\ \cdots \\ F_n \end{vmatrix} = \begin{vmatrix} 0 \\ F_2' \\ \cdots \\ \cdots \\ F_n' \end{vmatrix} \tag{3.2}$$

Iterating till the last node but one is freed; the free shape of the ring is then calculated. Figure 3-5 and Figure 3-6 illustrate this procedure.

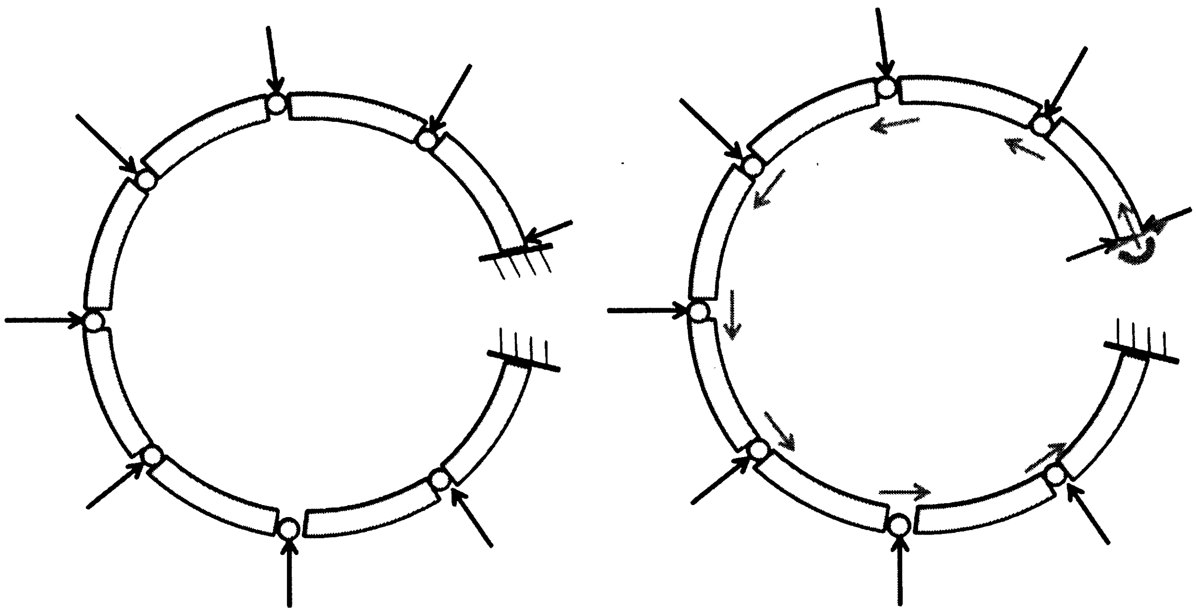

Figure 3-5 Free procedure 1: release restrain, add opposite force, solve displacement

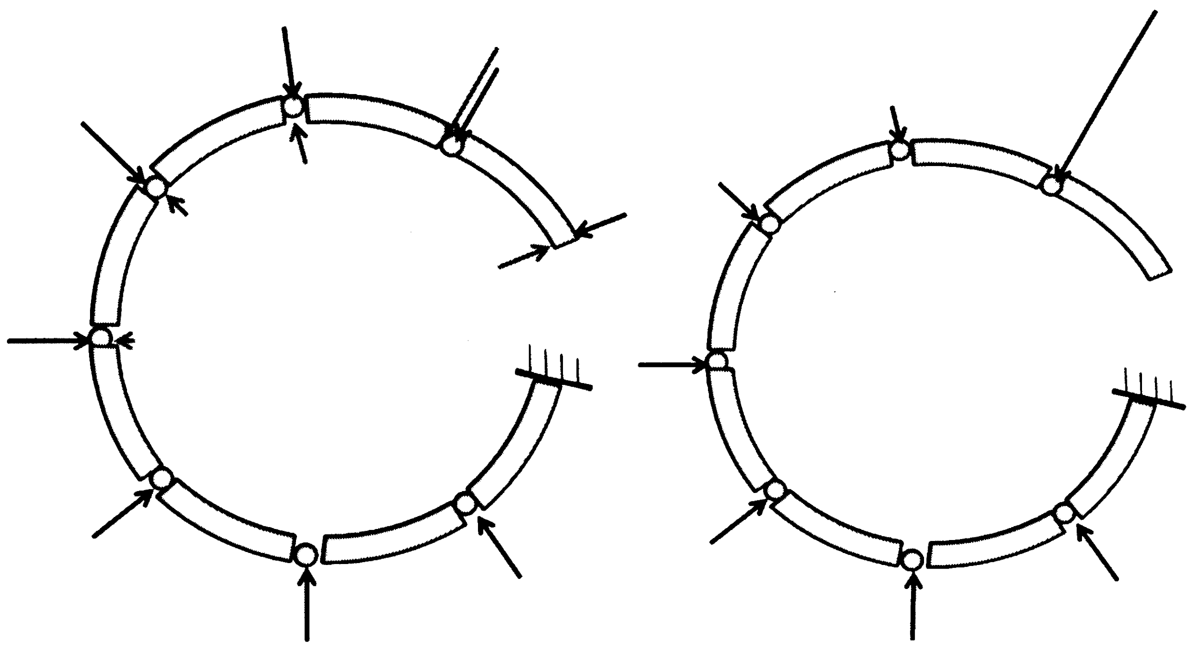

Figure 3-6 Free procedure 2: solve reaction load, update geometry and initial force

3.4 Fit Procedure

Now the free shape of the ring is known. The ring is totally released and has no external force or constrains. The purpose of fit procedure is to mount the ring into a nominal piston, preparing an initial state to interact with the bore. This fit procedure is the opposite way of free procedure.

One of the ring tips is constantly fixed. The node which is going to be fitted is allowed a displacement towards the center of the nominal bore. This displacement is give by the radius difference between nominal bore point and actual ring node point. The corresponding reaction load can be calculated:

$$\begin{vmatrix} K_{11} & K_{12} & & & 0 \\ K_{13} & K_{14}+K_{21} & K_{22} & & \\ & K_{23} & \cdots & & \\ & & & \cdots & K_{n3} \\ 0 & & & K_{n2} & K_{n4} \end{vmatrix} \begin{vmatrix} u_{01,1} \\ 0 \\ \cdots \\ \cdots \\ 0 \end{vmatrix} = \begin{vmatrix} F_{r1,1} \\ F_{r1,2} \\ \cdots \\ \cdots \\ 0 \end{vmatrix} \qquad (3.3)$$

But now we need to use the calculated reaction load to calculate the accurate displacement back. The reason is that the amount of given displacement mentioned above has a small circumferential direction component which is ignored in the last step purposely for convenient purpose. This step is actually serving as iteration to get a more precise displacement field. The new displacement will be used to update the coordinate rather. However, in the existing tool, the estimate displacement is used. This is the major improvement. Then the stiffness matrix is also updated. The reaction force will be used as initial force for the next iteration:

$$\begin{vmatrix} K'_{11} & K'_{12} & & & 0 \\ K'_{13} & K'_{14}+K'_{21} & K'_{22} & & \\ & K'_{23} & \cdots & & \\ & & & \cdots & K'_{n3} \\ 0 & & & K'_{n2} & K'_{n4} \end{vmatrix} \begin{vmatrix} 0 \\ u_{02,1} \\ \cdots \\ \cdots \\ 0 \end{vmatrix} = \begin{vmatrix} F_{r1,1} \\ F_{r2,1} \\ \cdots \\ \cdots \\ 0 \end{vmatrix} \qquad (3.4)$$

Iterating till the last node, the ring is fitted into the nominal bore. Figure 3-7 shows this procedure.

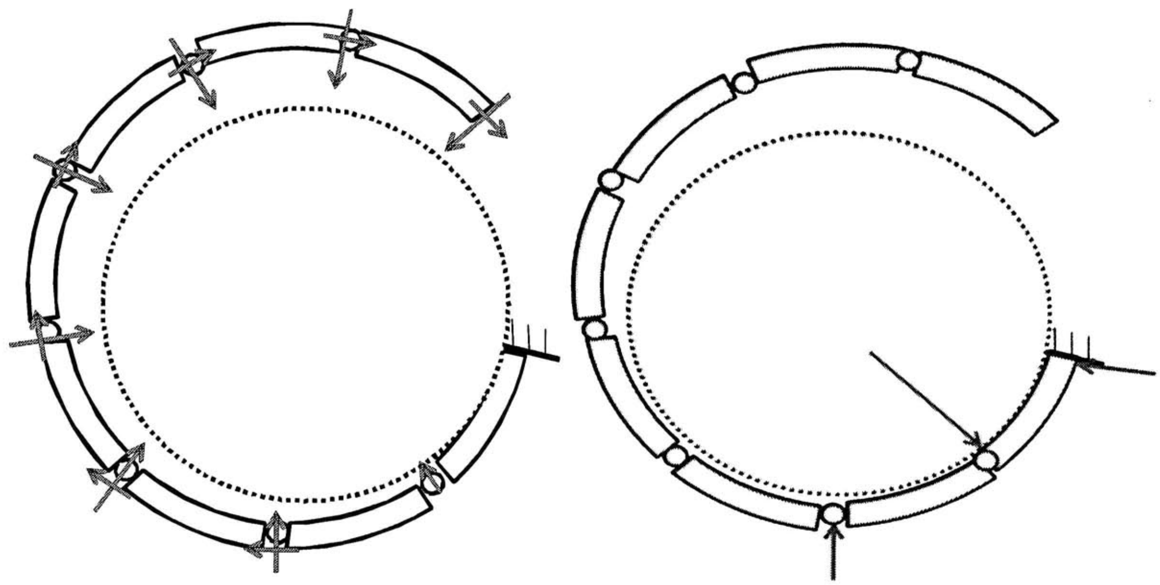

Figure 3-7 Fit procedure: solve displacement and reaction load, update geometry and initial force

There is fitting force wave propagation in this procedure. The absolute value of the propagation force decreases as the fitting process approaches to the other end of the ring tip as shown in Figure 3-8:

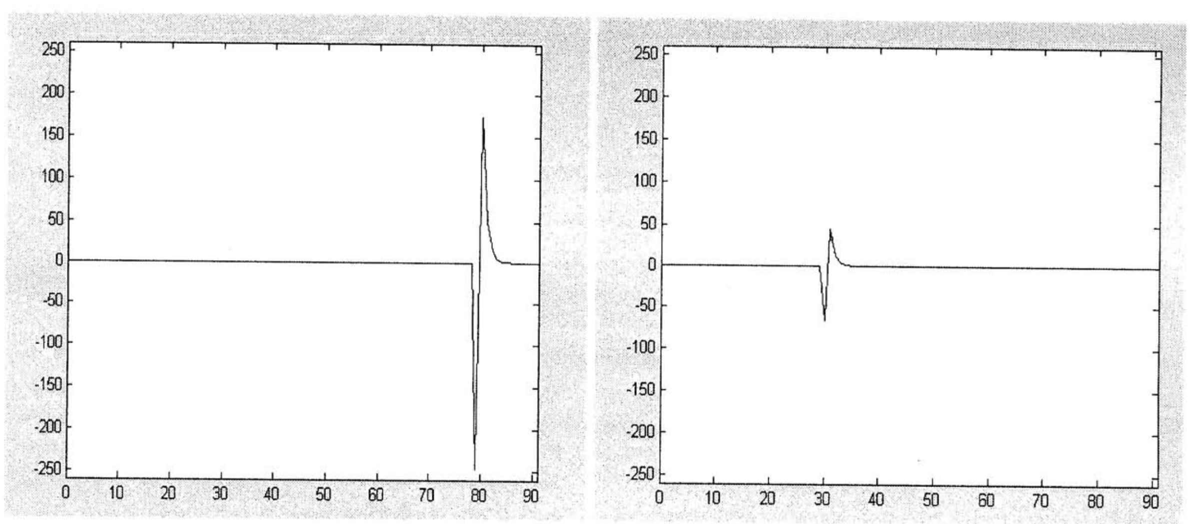

Figure 3-8 Fitting force marching, direction from right to left

3.5 The equivalence of Free and Fit procedure

These two procedures are designed to be equivalent and reversible. In another word, the initial ring shape and pressure distribution can be retrieved from performing fit procedure on the freed ring. There are two requirements to guarantee the reversibility of these two procedures.

First of all, the DOF set up of each node should be opposite in these two procedures, as shown in Figure 3-9:

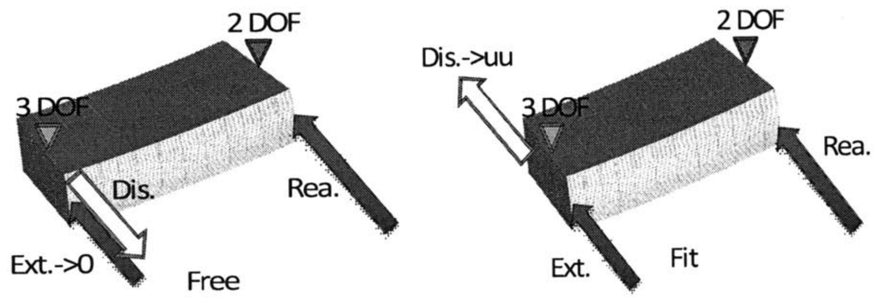

Figure 3-9 DOF set up (free vs. fit)

Secondly, the equation set up of these two procedures is equivalent, as show in table 3-1:

Free the ring	Fit the ring:
Nodes not freed:	Nodes been fit:
{x=0 (BC), y} {fx, fy}	{x=0 (BC), y} {fx, fy}
Nodes freed:	Node being fit:
{x', y'} {0, 0}	{x=xi (BC), yi} {0,0}
Solve displacement:	Nodes not been fit:
{y, x', y'}	{x', y'} {0, 0}
Solve reaction force:	Solve displacement:
{rx}	{y, yi, x', y'}
New displacement field:	Solve reaction force:
{x+x', y+y'}	{rx, rxi}
New force field:	New displacement field:
{fx+rx, fy}	{xi+x', y+yi+y'}
	New force field:
	{fx+rx, fyi+ryi}

Table 3-1 Equation set up (free vs. fit)

In order to validate the reversibility of these two procedures, the initial force and the fitting force are compared. As figure 3-10 shows that they are almost the same.

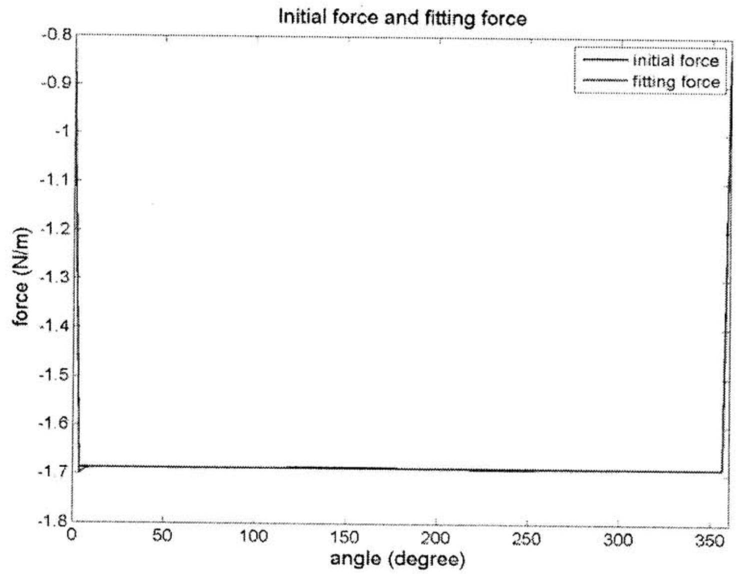

Figure 3-10 Initial force and fitting force comparing

The ring is also freed and fitted back in for many times, the difference between the initial force and the final fitting force is within acceptable range. See figure 3-11.

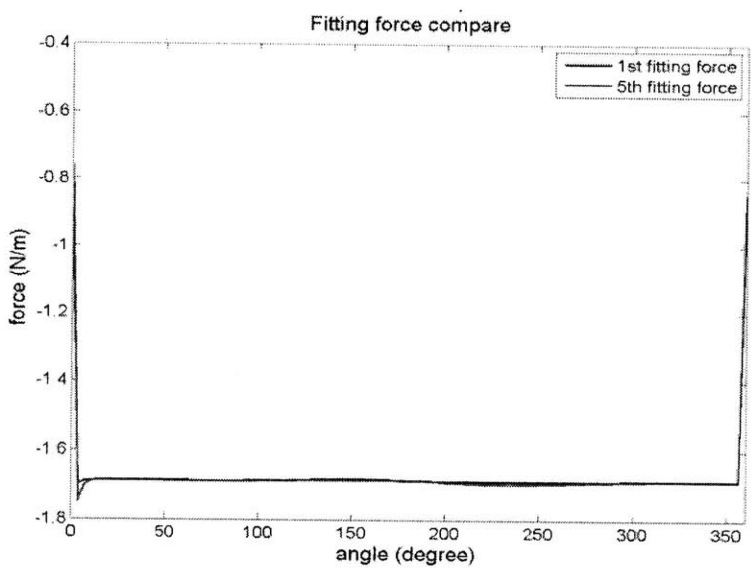

Figure 3-11 Initial force and fitting force after 5 times repeat comparing

3.6 Conclusions

In this chapter, a basic assumption of this thesis work is introduced that the curvature of the ring tips are the same in different ring states. Based on this assumption, the free and fit ring procedures are built up. They are different from the existing tool. Instead of fixing the ring back node to carry out the process, new method fixes one of the ring tip. This method also removed the symmetric ring assumption. The nominal bore therefore needs to be put at the tip location. The center of the bore is calculated using the first ring tip geometry information and the radius of the bore.

The detail iteration processes of free and fit procedure are explained along with the procedure of solving the corresponding equations. A fitting force propagation was found during the fit procedure. In order to explain the equivalence of fit and free procedure, how the DOF and equations set up are discussed. A repeat fit-free the ring back and forth experiment shows that they are mathematically reversible.

(This Page was intentionally left blank)

Chapter 4 Ring Bore Interaction

4.1 Introduction

There are many important piston ring design characters. For example, ring bore contact force, the clearance between ring and bore, curvature of the ring and ring stress distribution. All of these characters are of great interests. Therefore, a model which can simulate the interaction between the ring and the bore correctly needs to be chosen. It might take many situations into considerate such as solid contact friction, heat transfer, gas pressure and oil lubrication.

The real cylinder bore is not perfect rounded and smooth. The bias is due to the mechanical and thermal distortion, which is called bore distortion. This imperfection makes the behavior of the ring much more complicated. For example, some parts of the ring might tilt away or against the bore due to the distorted curvature of the bore. The region that the ring tilt away may lose contact which will harm the gas sealing and oil control functions of the ring cause more gas blow by or oil consumption. The region that the ring tilt against the bore may generate huge contact force with will cause serious wearing of the ring that will decrease the durability of the engine. Therefore it is necessary to analyze the ring behavior while taking the bore distortion into consideration.

Several sub-models such as asperity contact force model, hydrodynamics pressure model are used in the ring bore interaction analysis. We call it conformability analysis because the characters we calculated such as clearance and contact force are ways to describe how well the piston ring conforms to the cylinder bore.

It is also important to know the stress distribution of the ring. The sensitivity of the ring tips sheds light to the credibility of the main ring tip curvature assumption in this thesis. It is also with many interests to exam how the ring behaves when it is rotating or moving reciprocates in the bore. If the space between the ring and the bore is partially lubricated rather than fully flooded, how the contact force will change is also discussed in this chapter.

4.2 Bore Distortion

Because of certain mechanical and thermal reasons, there will be distortions which make the cylinder bore not perfect rounded. These distortions have always been an important subject to investigate because they play a big role in combustion gas sealing, friction control and oil consumption.

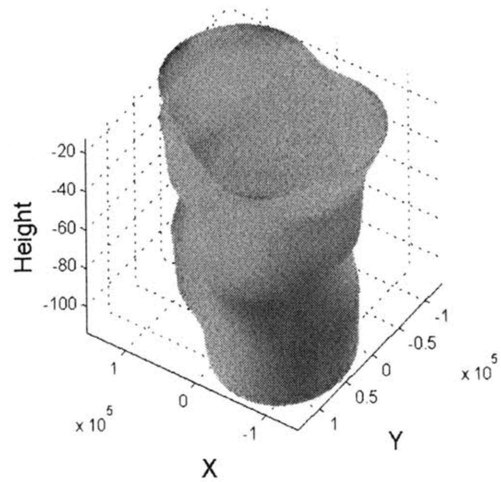

Figure 4-1 Cylinder bore distortion [2]

The bore distortion can be expressed as a serial:

$$dB = \delta_2 \cos[2(\theta + \alpha_2)] + \delta_3 \cos[3(\theta + \alpha_3)] + \delta_4 \cos[2(\theta + \alpha_4)] \quad (4.1)$$

Where dB is the bore distortion, θ is the circumferential location, δi is the magnitude of the ith order bore distortion, and α is the corresponding phase angle relative to the gap location [2].

4.3 Asperity contact force model

The Asperity contact pressure between the mounted ring and the distorted bore is modeled theoretically by Greenwood and Tripp (1971) [15]. A simple numerical correlation of this theory provided by Hu is used here. The asperity contact force can be expressed as: [16]

$$p_c = \begin{cases} K \cdot E/(1-\nu^2) \cdot A(\Omega - h/\sigma)^Z & h/\sigma \le \Omega \\ 0 & h/\sigma > \Omega \end{cases} \tag{4.2}$$

Where p_c is the asperity contact pressure, σ is the combined surface roughness, h is the nominal clearance between the ring running surface and the bore, z and A are the correlation constant, K is surface-asperity related characteristics and E is Young's module.

Whenever there is no oil in between the ring running surface and the bore, the asperity contact force model is used. These regions are called dry regions. If the clearance between the ring running surface and the bore is larger than 4σ, it will lose contact which means there is asperity contact force [17]. If the clearance is very small sometime it can be negative, there will be large contact force. There is a regulation mechanism to prevent it from happening.

4.4 Hydrodynamics Lubrication Model

If there is lubrication oil in between the ring running surface and the bore, a simplified hydrodynamics lubrication model [30,31] will be used here to calculate the hydro-pressure. These regions are called wet regions. As shown in figure 4-2:

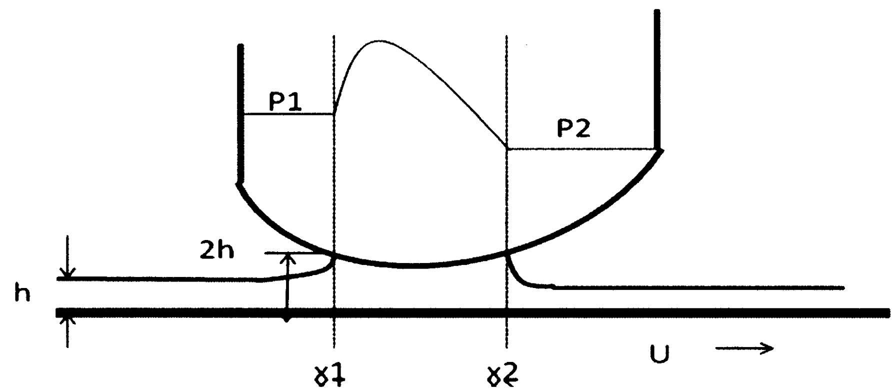

Figure 4-2 Simple Hydrodynamics Lubrication Model

Where p1, p2 are the gas pressure, U is the sliding speed, h is the local clearance. Then the volumetric flow rate can be calculated as [20]:

$$q = \frac{\int_{x_1}^{x_2} \frac{6\mu U}{h^2} dx - (p_2 - p_1)}{\int_{x_1}^{x_2} \frac{12\mu}{h^3} dx} \tag{4.3}$$

The pressure distribution can be written as:

$$\frac{\partial p}{\partial x} = \frac{12\mu}{h^3}\left(\frac{U}{2}h - q\right) \tag{4.4}$$

Then the integral of the wet region can be calculated to contribute together with the asperity contact force.

4.5 Conformability Calculation Results Analysis

Here a theoretical symmetric ring with symmetric initial pressure distribution is taken as an example for the first stage of calculation.

Contact force distribution [18]: It shows the contact force between the running surface of the ring and the cylinder bore in radius direction. As shown in figure 4-3:

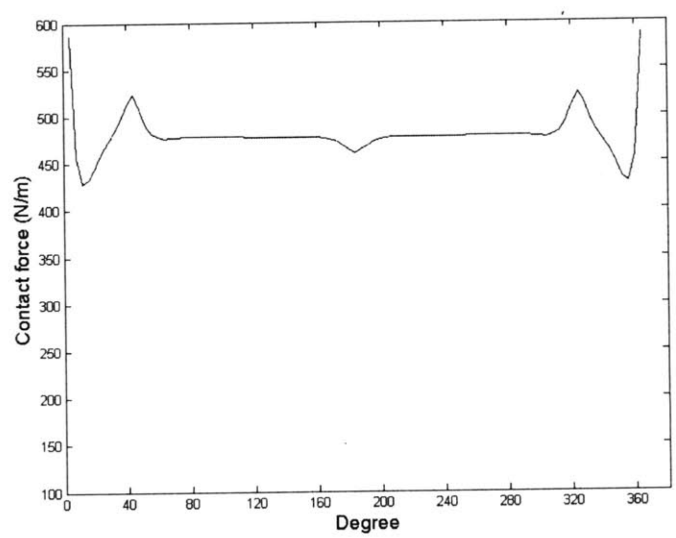

Figure 4-3 Contact force in radius direction

Clearance [19]: It shows the clearance between the running surface of the ring and the cylinder bore in radius direction. As shown in figure 4-4:

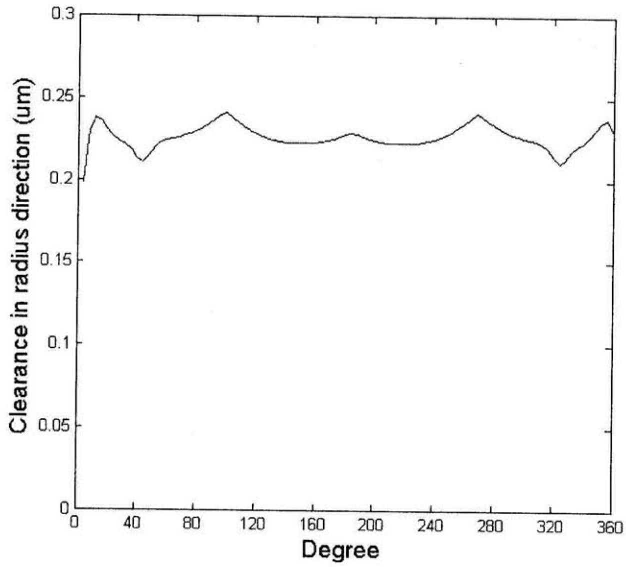

Figure 4-4 Ring bore clearance in radius direction

Piston ring stress [2]: It shows the stress distribution on the ring cross section on ID and OD. As shown in figure 4-5.

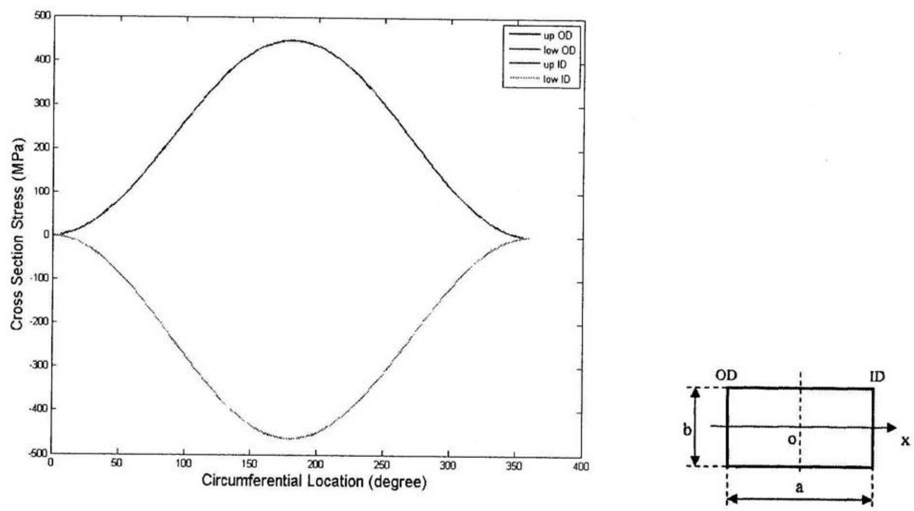

Figure 4-5 Cross section stress distribution and the definition of OD/ID

Piston ring cross section forces [2]: There is no internal force at the ring tips. The internal force in radius direction (shown in figure 4-6 with green line) and the bending moment in radius direction (shown in figure 4-7 with blue line) reach its maximum value at ring back. The internal force in circumferential direction (shown in figure 4-6 with blue line) reached its minimum value at the ring back.

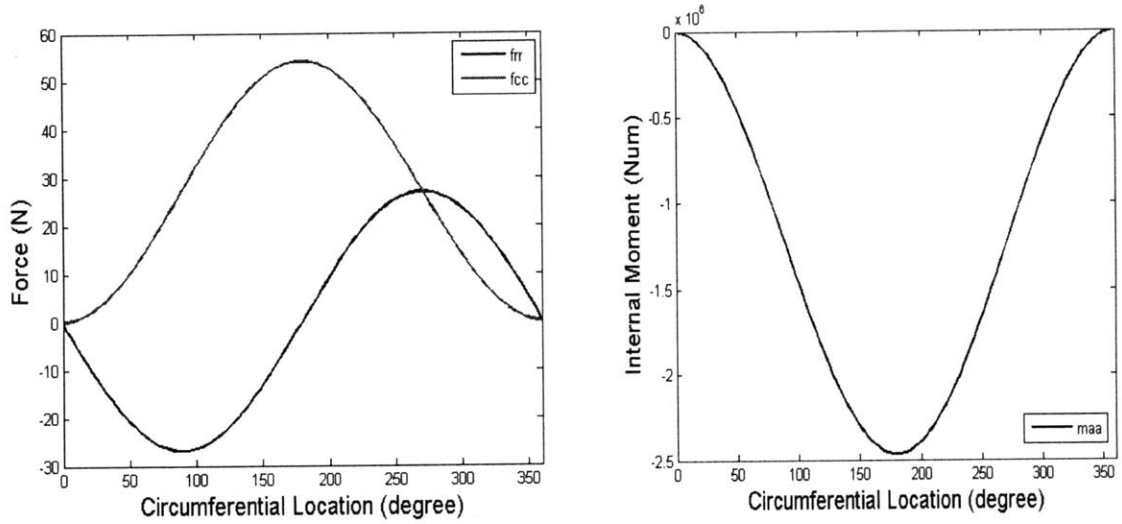

Figure 4-6 Internal forces and moment along the ring

Piston ring curvature: As shown in Figure 4-7.

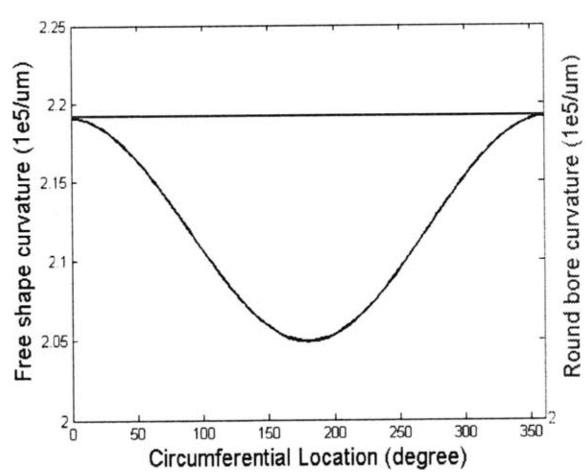

Figure 4-7 Curvature comparing between freed ring and nominal bore

4.6 Ring Rotation and Reciprocating Moving

To simulate the rotation of the ring within the distorted bore is a reasonable way to show the influence of distortion to the contact force. Instead of changing the actual ring position, the phase of the bore distortion is changed for a whole circle.

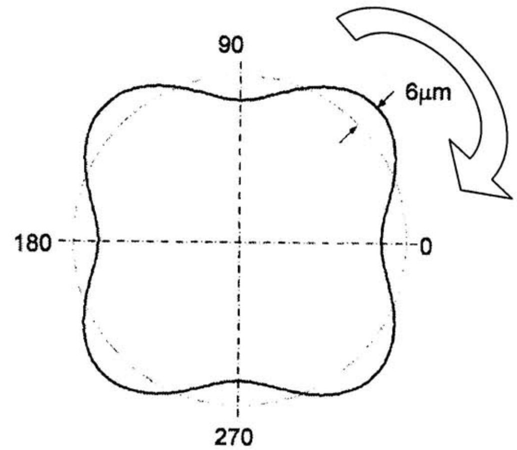

Figure 4-8 Changing distortion phases to simulate rotating effect of the ring

Figure 4-9 shows the contact force of two different phase positions of the ring after it is released in a distorted bore.

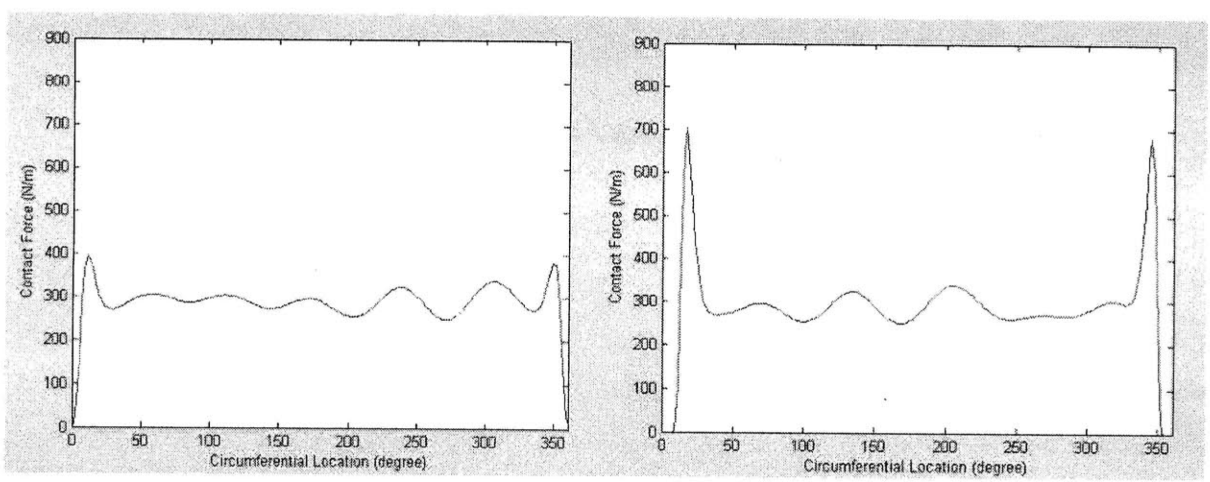

Figure 4-9 Contact force at phasce 30 and phase 100

To simulate the piston ring moving reciprocate in a distorted bore is another way the show not only the influence from the distortion but also from the CA. The working gas pressure is different from each CA, and the temperature is also different.

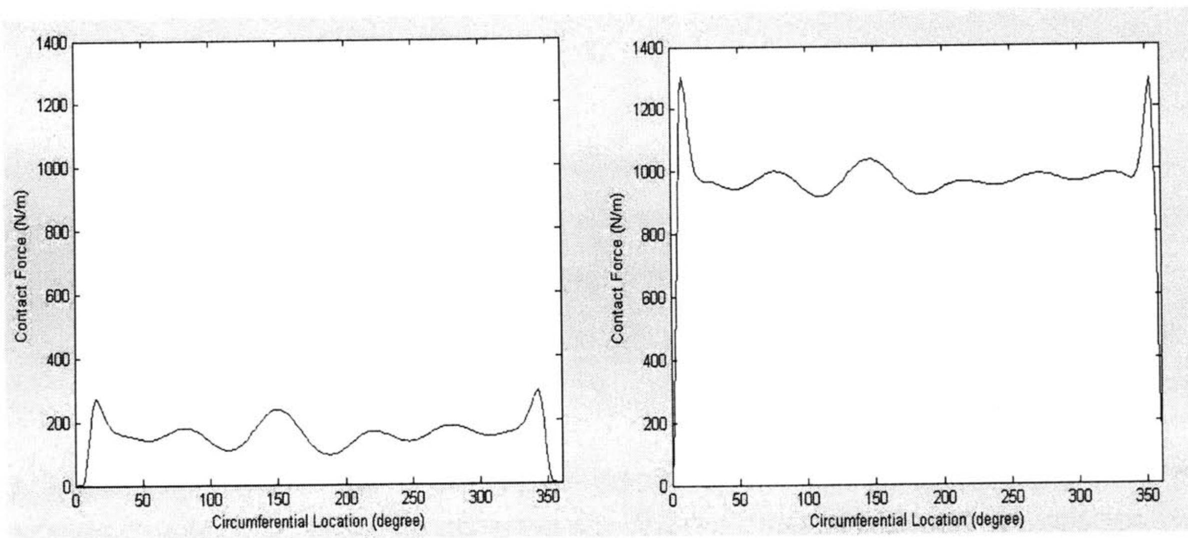

Figure 4-10 Contact force at CA 0 and CA 200

4.7 Influence from the roughness and partial wetting

The asperity contact force model takes roughness as a critiria. If the clearance is bigger than four times of roughness, it reduces to zero. So roughness plays an important role in comformability analysis. Figure 4-11 shows the different contact forces due to different ring bore surface roughness. As we can see, the smoother the cylinder bore is, the shaper the contact force is; the rougher the cylinder bore is, the smoother the contact force is.

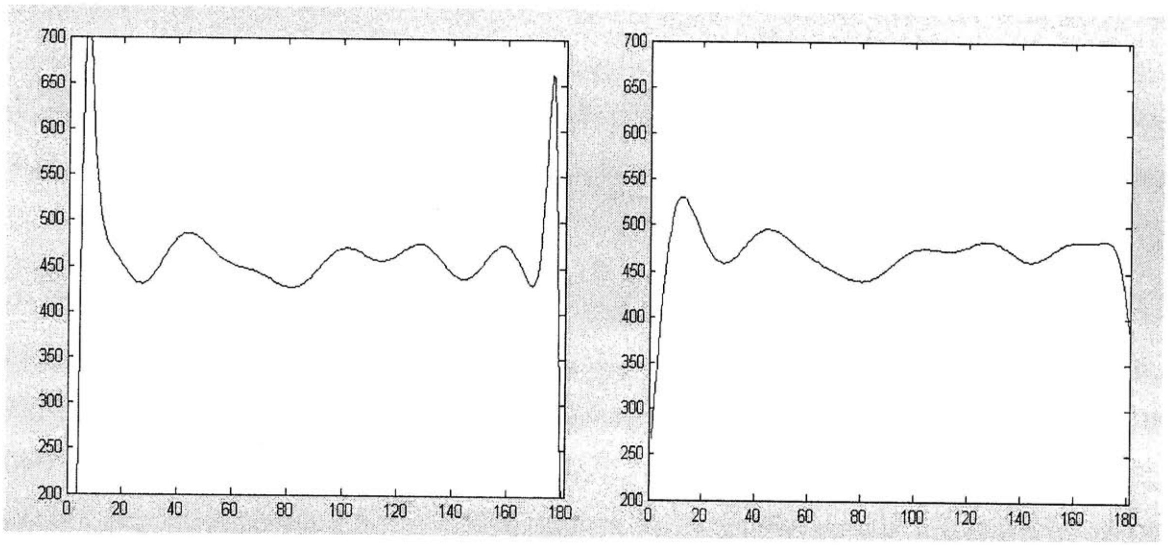

Figure 4-11 Contact force with different roughness (smaller vs. bigger)

If the lubrication oil is filled in between the cylinder and the bore, the hydrodynamics pressure will be generated. This pressure pushes the ring away from the bore, the clearance between the ring and the bore will be increased. Therefore the asperity contact force will be reduced. If some regions have too much oil, the ring will eventually lose contact with the bore at those regions.

The purpose here is to observe how the distribution of the oil does influence to the asperity contact pressure. The ring is divided into 8 regions along the circumferential direction. Some of the regions were chosen to be dry, which means the oil film thickness is zero. The other regions are filled with oil with given thickness. As shown in Figures 4-12 and 4-13, it is obvious that the contact force will be reduced in those regions filled with more oil.

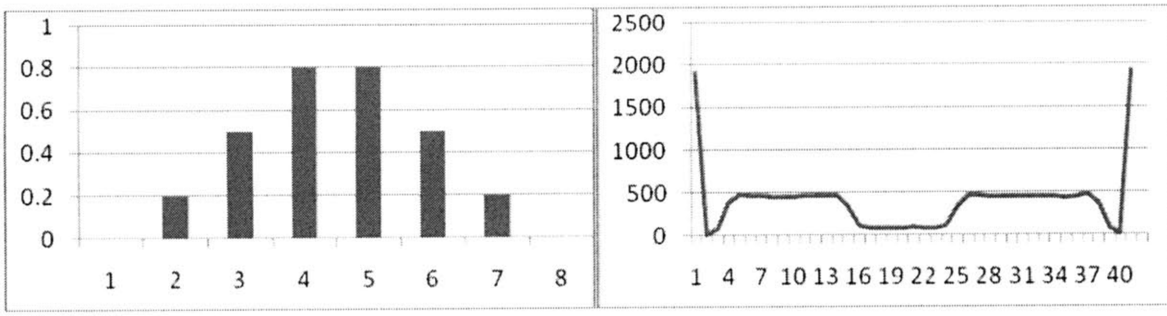

Figure 4-12 Oil film thickness and the contact force distribution 1

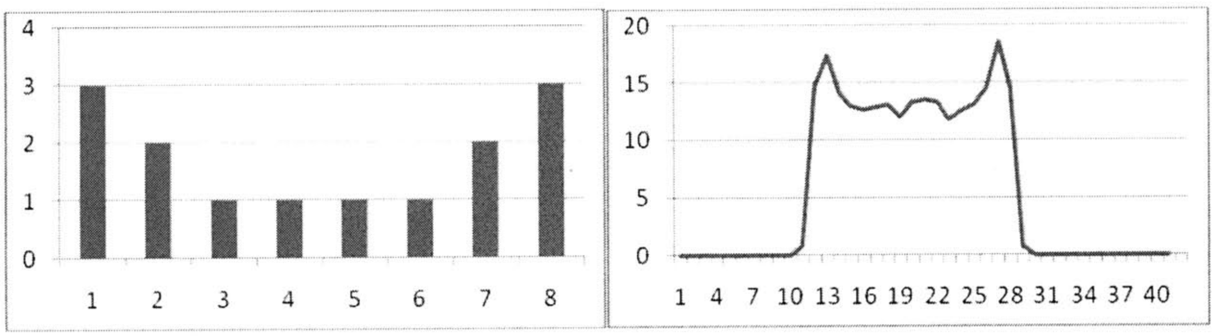

Figure 4-13 Oil film thickness and the contact force distribution 2

4.8 Conclusions

In this chapter, a serial is used to describe the bore distortion. Asperity contact force model and hydrodynamics lubrication model are introduced which will be used in the conformability calculation. The basic idea is that asperity contact force will be generated where the clearance is smaller. The hydrodynamics force will be generated where the space between the ring running surface and the piston bore is filled with oil and the piston has a sliding speed.

The conformability calculation gives the information like contact force, clearance, ring cross section stress and ring curvature. The phase of the bore distortion is changed to simulating the rotation of the ring within the bore. As the ring moving with the CA vertically in the cylinder, we can see the contact force changes with the chamber gas pressure, gas temperature and the instantaneous bore distortion information. If the region is wetted by oil, the asperity contact force will decrease. If the oil film is thick enough, the ring will lose contact with the bore.

Chapter 5 Case Study

5.1 Introduction

This chapter will go through a real case to show how the new piston ring design tool works. The task here is to calculate the ring bore contact force distribution from a set of measured ovality ring data. Then the calculated contact force will be compared with the theoretical initial force distribution in the design stage. If the new tool works well, these two results should be similar.

Our goal is to design a way of simulation starting from measured ovality data and ending with calculating contact force. The new tool can use any type of ring under arbitrary pressure distribution as input; in this case the measured ovality data is the input. The first challenge here is that the measure data is very noisy. A filter must be developed first to make the data smoother.

As mentioned before the ring tips are very sensitive parts of the ring. Different ways of filtering can result in different shapes of ring tips. Since the data are obvious asymmetric, we are going to fix the ring tip node to carry out our simulation. Thus the basic ring tip curvature assumption must be met. The second challenge is to choose a proper filter which can smoother the measure data in the mean time make the curvature at the ring tip equals to the nominal bore.

After the input data are prepared, the ovality ring is freed first to generate free ring. This free shape is fitted into a nominal bore. Then the conformability calculation can be carried out. The result will be compared with the theoretical one.

There are three types of ovality: Negative, Positive and Zero. Negative ovality means the diameter goes through the closed ovality ring gap and the ring back is smaller than the diameter in the other vertical direction. Positive means larger and Zero means they are the same. The comparisons of contact force, fitting force, clearance and curvature of these three types of ovality could be a good inspiration.

5.2 Measure Ovality Shape Filter

The measured raw ovality data is noisy as shown in the figure 5-1. Obviously a filter is needed to smooth the data. There are many choices of filter. However, only the filter which can make the curvatures near the ring tips equal to the nominal bore is the type of filter we want. This is due to the basic assumption in this work. We found out the following method can fulfill our needs.

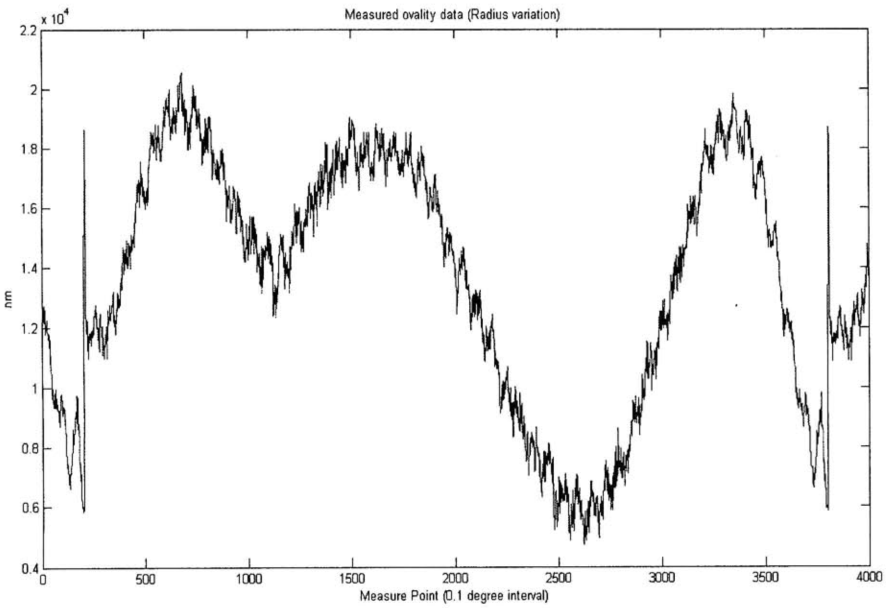

Figure 5-1 A sample measured ovality data

Step 1: In this case the measure ovality data is the variation of radius. First of all, the variation data are shifted to make the variation at one of the ring tip equals to zero. See figure 5-2.

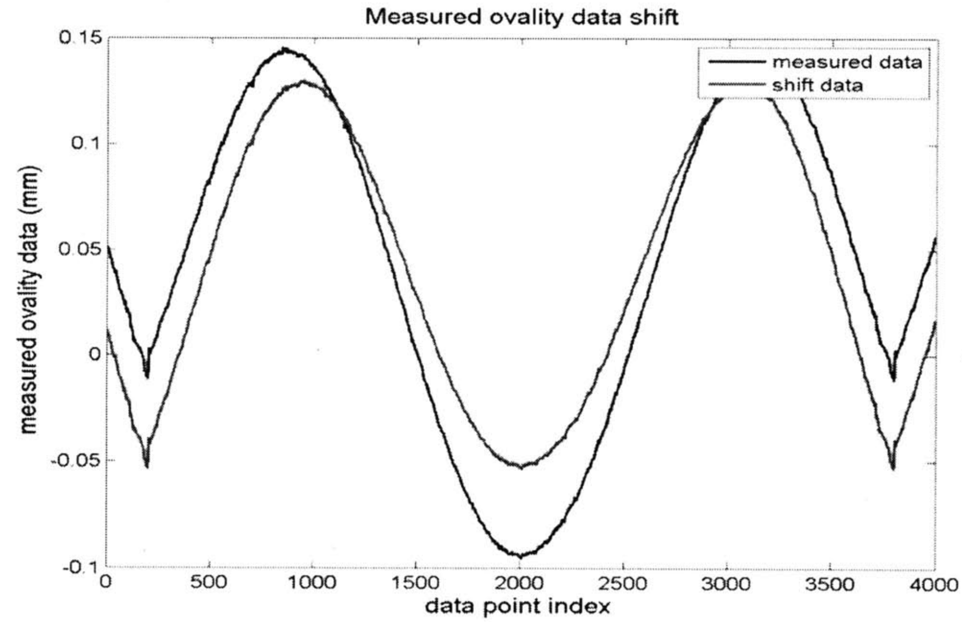

Figure5-2 Measured variation data shifted to zero at the ring tip

Step 2: Reasonable amount of node points are selected evenly from the shifted data. Then a spline filter is operated on these sample data point to give us a much smoother data. See figure 5-3.

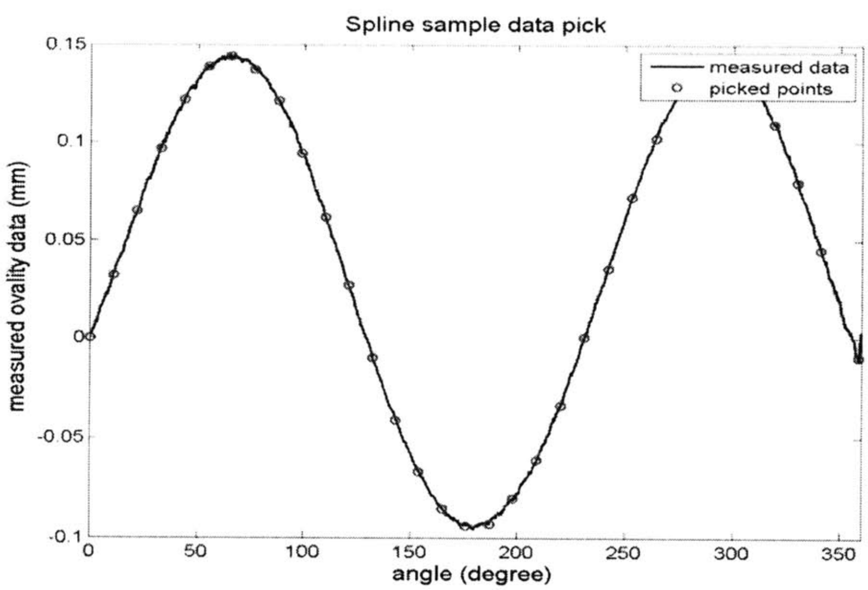

Figure 5-3 Sample data points choose and spline filter

Step 3: However, at this step, we cannot guarantee the curvature at the ring tips are equal to nominal bore. Besides, there are still many high frequency noises in the spline filtered data. Spline filter is used to makes the curvatures at the tips equal to the nominal bore. FFT filter is chosen to eliminate these waves. Since FFT filter can only be operated on periodical data, we flip the data to make it periodical. As shown in figure 5-4, the left part of the curve is the original data. We change the sign of the data, flip them from side to side, and move them to the right, then connect them with the original one. Now the data are periodical.

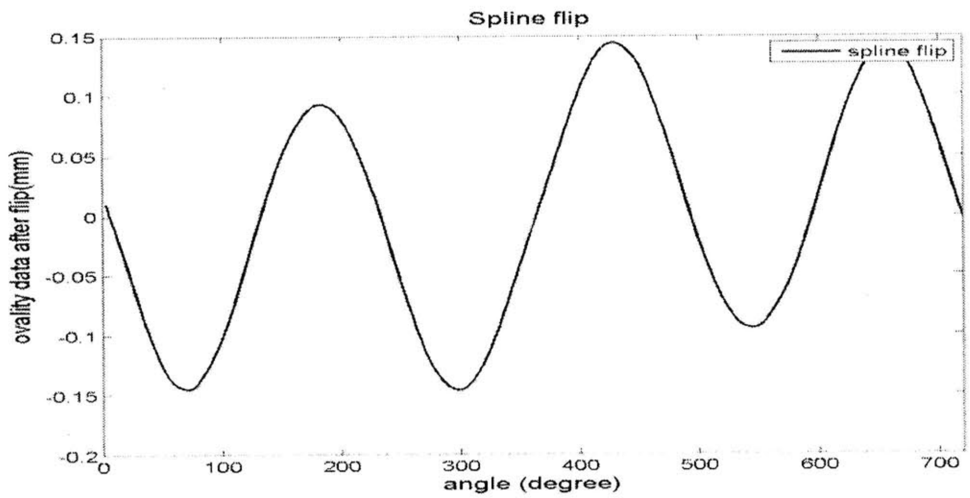

Figure 5-4 Flip the data to make it periodical

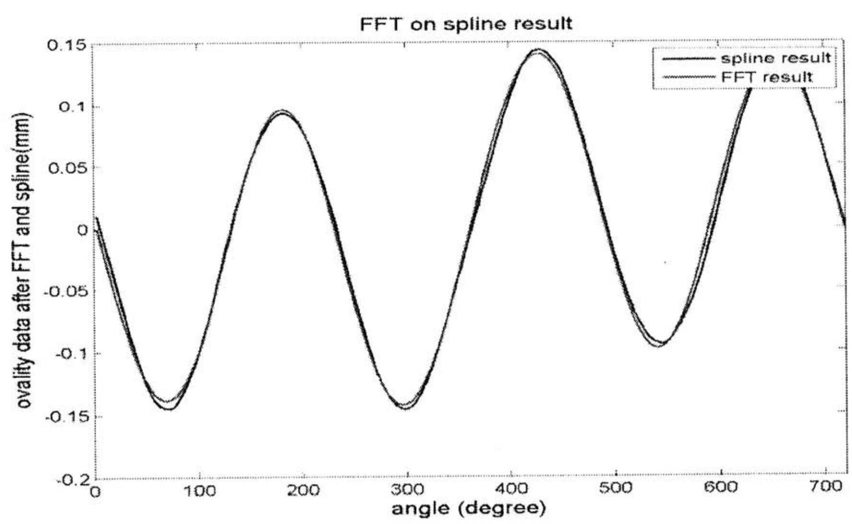

Figure 5-5 FFT Filter

A spline-FFT filtered data is prepared for the following calculation. Figure 5-5 shows the difference between spline filtered data and spline-FFT filtered data.

There are three types of ovality ring as mentions in the introduction part. They are shown in the red curve in figure 5-6. The data used here is the spline-FFT filtered data. It is interesting to notice that the flipped part, which is the blue curve, turns out to be an opposite ovality ring type to the original red one.

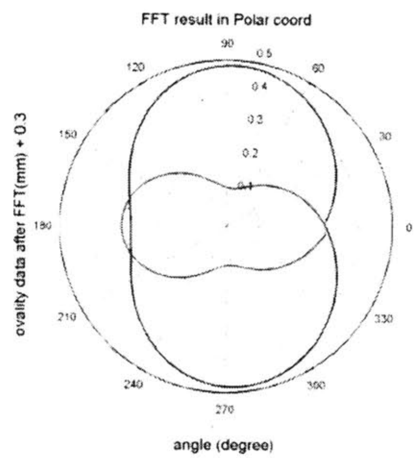

Positive ovality ring

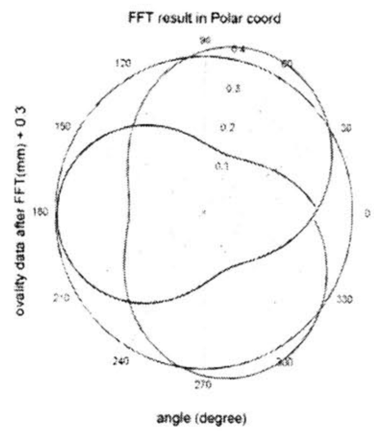

Negative ovality ring

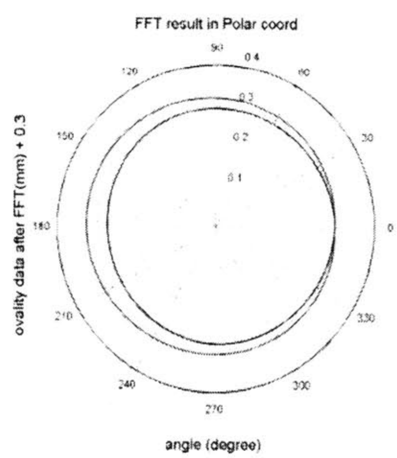

Zero ovality ring

Figure 5-6 Negative/Zero/Positive ovality ring

5.3 Result Analysis

Curvature of ring ovality shape and the ring free shape:

As shown in figure 5-7 and figure 5-8, the curvatures near ring tips change little from ovality to free shape. It's a strong proof of our assumption.

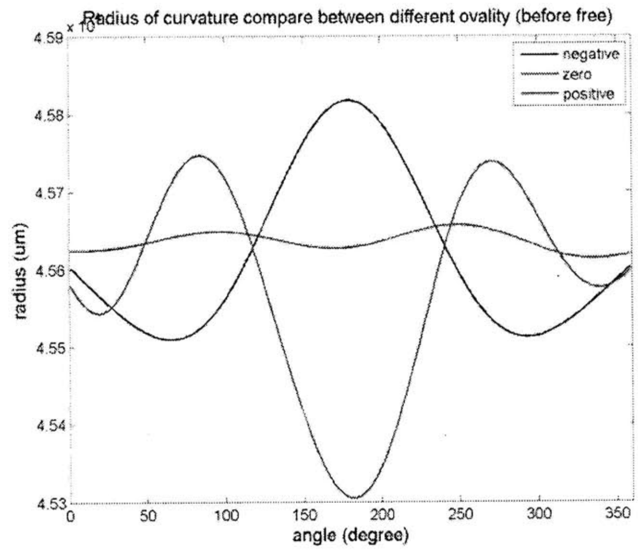

Figure 5-7 Negative/Zero/Positive ovality ring free shape curvature

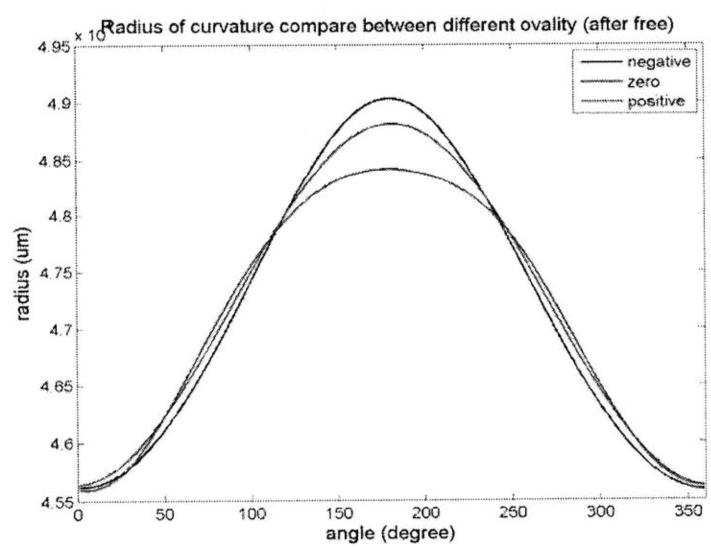

Figure 5-8 Negative/Zero/Positive ovality ring free shape curvature

Fitting force:

Fixing one of the ring tips, the ring is fitted into the nominal bore. Figure 5-9 shows the final fitting force on the ring. In order to prove that the fitting procedure does not depend on the choice of direction, we fix another ring tip, correspondently move the bore position next to that ring tip then fit the ring. Comparing these two fitting forces as shown in figure 5-10 we can find they are almost the same. Thus the fitting procedure can be said as direction independence. This is a strong prove to the removal of symmetric assumption in the new tool.

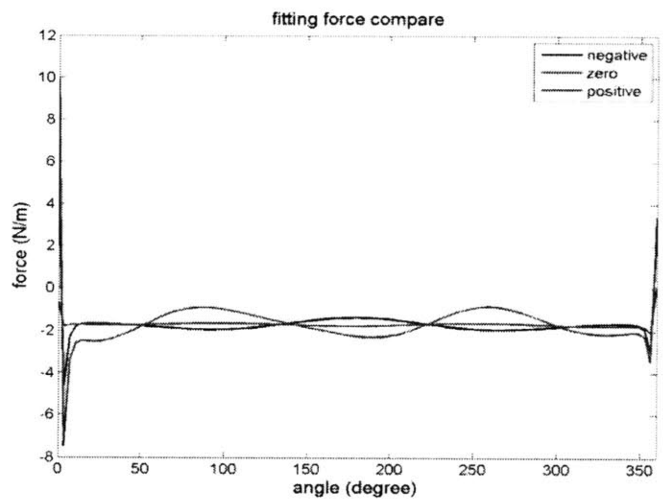

Figure 5-9 Freed Negative/Zero/Positive ring fitting force

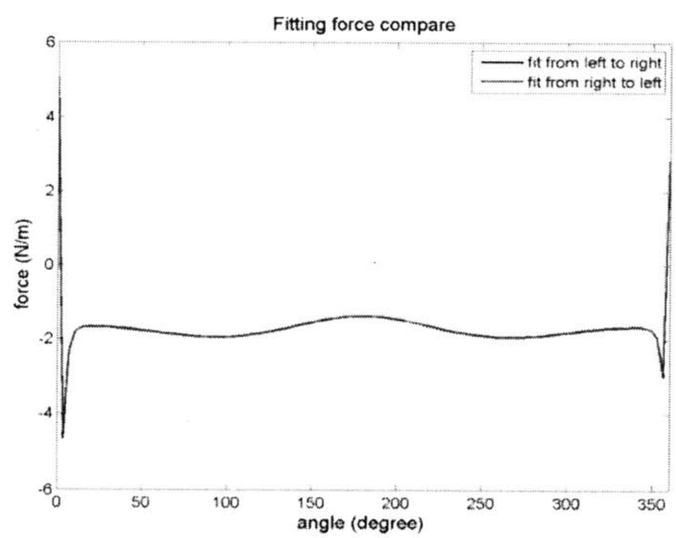

Figure 5-10 Comparing he fitting force fit from different tip of the ring

Ring bore clearance and contact force:

Clearance is shown in figure 5-11 and contact force in figure 5-12. As we can see, the bigger the clearance is, the smaller the contact force. In some cases the ring tips lose contact with the bore (tilt away) therefore there is no external force near the tips and the curvatures remains the same as its free state.

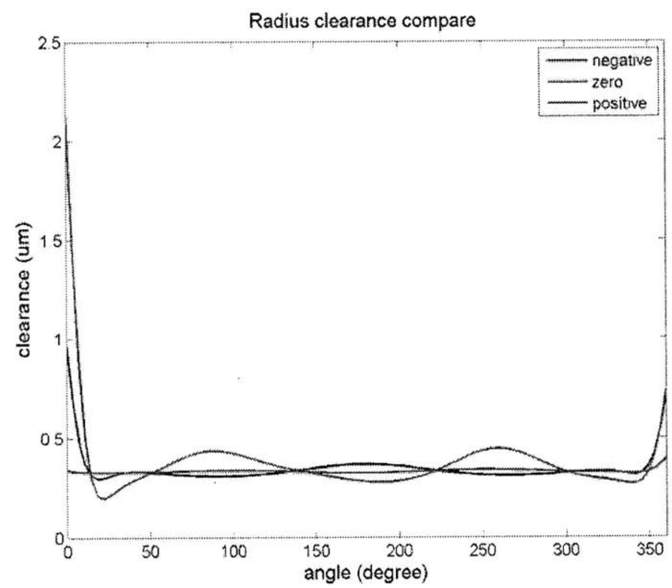

Figure 5-11 Radius clearance between the Negative/Zero/Positive ring and the bore

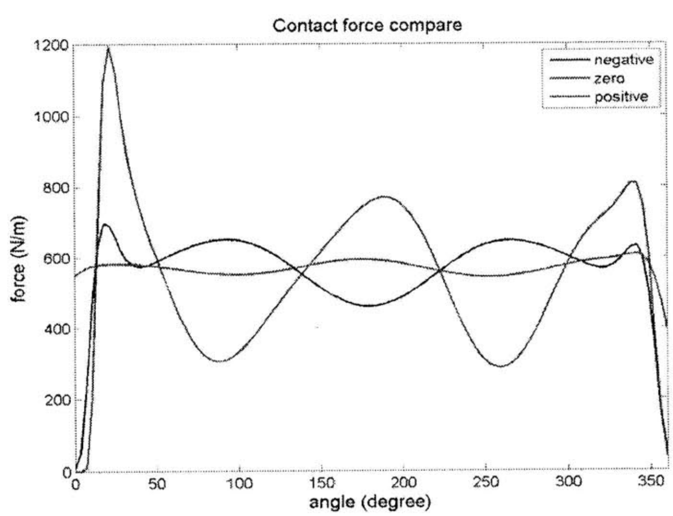

Figure 5-12 Contact force comparing of Negative/Zero/Positive ring

Contact force and initial force distribution in design stage comparison:

As shown in figure 5-13, the calculated contact force can capture the major characteristics of the initial force distribution. Especially when the initial force is distributed in bigger wave length as cosine wave, for example, the zero ovality ring. The reason is that those high frequency waves are filtered by the FFT filter mentioned above.

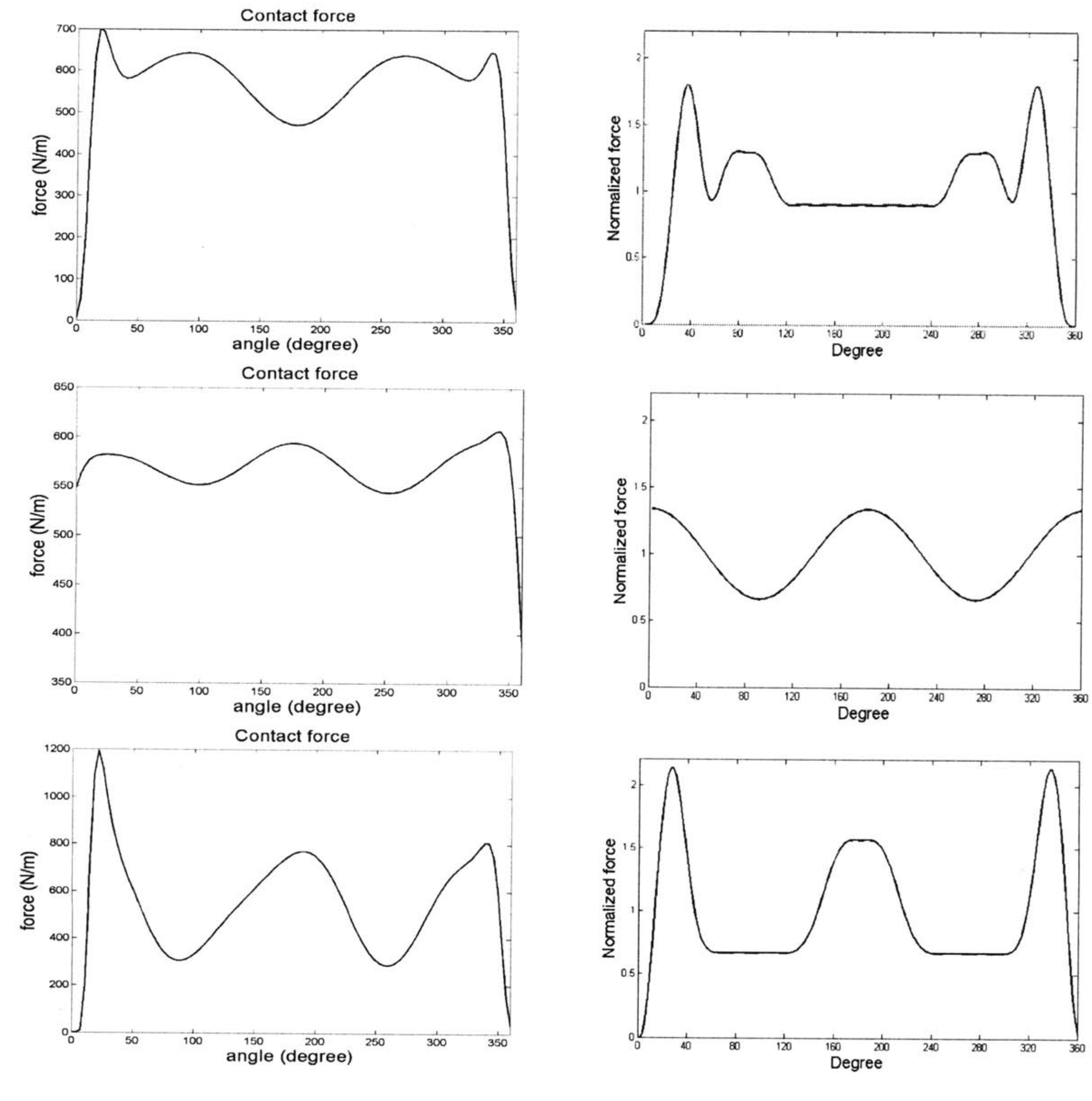

Calculated contact force Desired contact force

Figure 5-13 Comparing the calculated contact force with the designed theoretical contact force

5.4 Conclusions

In this chapter, the model we built is used on a real industry ring design case. The measured ovality raw data is noisy and a proper type of filter is created. There are two purpose of this filter: First, to eliminate those high frequency noises in the data make them smoother enough to calculate; second, to make the curvature and the ring tip equal to the nominal bore. A spline-FFT filter can lead to good result.

The filtered asymmetric ovality shape is freed node by node, results in a free ring. This freed ring is fitted onto a nominal bore then released to interact with the distorted bore. The conformability calculation is preformed on three different types of rings: negative/zero/positive ovality rings. The contact force, clearance and curvature of the rings are compared. The calculated contact force is similar to the designed initial force distribution which means the method of calculating contact force from measured ovality data is valid.

Chapter 6 Summary

In order to enable us to use the industry measured piston ring ovality data to simulate the behavior of ring bore interaction, a model needs to be built up to calculate ring bore contact force and clearance using these ovality data. This model should also be able to connect different types of ring working conditions together such as free ring, ovality ring and conformability ring.

The measure raw data is very noisy and asymmetric. A proper filter is needed to filter the raw data to make them ready for calculation. The choice of the filter is not arbitrary; it depends on certain boundary conditions. By experiments this boundary condition is found to be suitable: ring tip curvature is the same as the nominal bore.

The filtered ovality data is ready. First step is to fix one of the ring tips then free the ring node by node using FEM. After all the forces and constrains are released, the ring free shape is calculated. The second step is to hold the same ring tip, put the nominal bore in a proper position, and fit the ring back to the nominal circle node by node. By doing this the ring can be prepared to interact with the distorted bore without large displacement. In order to validate these free and fit procedure are physically reasonable, an equivalent test is carried out to prove they are correct: free and fit the ring back and forth the fitting force and the initial force are the same; the fitting forces are the same by fitting the ring from each tips. Finally, the fitted ring is ready to interact with the bore. The contact force, clearance, ring tension and curvature are calculated.

The measured ovality ring is a real industry design which means the free shape of this ring is designed to have a desired pressure distribution with the nominal bore once it is put into the cylinder. This means the ring is made following the designed free shape. The free shape calculated by the free procedure above matches this designed free shape. The contact force calculated by the fit procedure above matches this desired contact force. These two results proved that method in this work is correct. Besides, this model provides a network of calculating these ring working states, as shown in figure 5-1.

During the experiments, some interesting phenomenal was noticed. Ring tips are critical regions, they can contribute huge contact force if they are tilting against the bore or they can lose contact if they are tilting away. Bore position is critical, if the position didn't obey the basic assumption in this work, ring tip curvature is always the same as the nominal bore, and the result would be unreasonable. Ring tips are also sensitive to the way their shapes are filtered from raw data, if the filter is off the assumption, the result might also be far away from expecting.

Certain parameters were changed to show how the ring bore interaction changes with them, such as roughness and oil wetting condition. The piston ring was also forced to move, both rotating and reciprocating moving in the cylinder. The resulted contact forces are analyzed.

All of these new features and experiments are integrated into a efficiency code package. Many different ways of ring design can be chosen freely. This work has appreciating practical value in the automobile industry.

References

1. Nakada,M., "Piston and Piston Ring Tribology and Fuel Economy", Proceedings of Internal Tribology Conferece, Yokohama, 1993.
2. Liang, L., "Modeling the Performance of the Piston Ring-Pack with Consideration of Non-Axisymmetric Characteristics of the Power Cylinder System in Internal Combustion Engines", 2005.
3. Federal MOGUL, "Piston Ring Handbook", Federal-Mogul Burscheild GmbH, 2008.
4. RIKEN Corporation, "Piston Ring Museum", RIKEN Corporation, 2008.
5. International Organization for Standardization, "Piston Rings and Pins", ISO, 2006.
6. Tian, T., 2002, "Dynamic Behaviors of Piston Rings and Their Practical Impact. Part 1: Ring Flutter and Ring Collapse and Their Effects on Gas Flow and Oil Transport," Proc IMechE, Part J: Journal of Engineering Tribology, Vol. 216, pp. 209-227.
7. Tian, T., 2002, "Dynamic Behaviors of Piston Rings and Their Practical Impact. Part 2: Oil Transport, Friction, and Wear of Ring/Liner Interface and the Effects of Piston and Ring Dynamics," Proc IMechE, Part J: Journal of Engineering Tribology, Vol. 216, pp. 229-247.
8. Liu, L., Tian, T., and Rabute, R., 2003, "Development and Application of an Analytical Tool for Piston Ring Design," SAE Paper 2003-01-3112.
9. Liu, L., Tian, T., 2004, "A Three-Dimensional Model for Piston Ring-Pack Dynamics and Blow-by Gas Flow," ASME ICE Fall Technical Conference, ICE 2004-968.
10. James, M.G., Stephen, P.T., *Mechanics of Material*, PWS Pub. Co., 2008.
11. Ejakov, M. A., Schock, H. J., and Brombolich, L. J., 1998, "Modeling of Ring Twist for an IC Engine," SAE Paper 982693.
12. Prescott, J., *Applied Elasticity,* Dover Publication Inc. New York, 1925.
13. Pan, Z., *Finite Element Analysis and its Applications*, Tsinghua University Press, 2001
14. Tirupathi, R. C., Ashok D.B., *Introduction to Finite Elements in Engineering*, PRENTICE HALL, 1991.
15. Hu, Y., Cheng, H. S., Arai, T., Kobayashi, Y., and Aoyama, S., 1993, "Numerical Simulation of Piston Ring in Mixed Lubrication - A Nonaxisymmetrical Analysis," ASME Journal of Tribology, 93-Trib-9.

16. Greenwood, J. A., and Tripp, J. H., 1971, "The Contact of Two Nominally Flat Surfaces," Proc. Inst. Mech. Engrs., Vol. 185, p.62 5.
17. Sun, D. C., "A Thermal Elastica Theory of Piston-Ring and Cylinder-Bore Contact," ASME Journal of Applied Mechanics, Vol.58, pp. 141-153, 1991.
18. Timoshenko, S., and Lessells, J. M., *Applied Elasticity,* Westinghouse Press, 1925.
19. Feodosyev, V. *I., Selected Problems and Questions in Strength of Materials,* Mir Publishers, 1977.
20. Tian, T., 1994, "A note on hydrodynamic friction coefficient and minimum film thichness of piston ring", Sloan Automotive Laboratory.